NBUJPS
NBU Journal of Plant Sciences

ISSN No. 0974-6927
Vol. 17 (2025), pp. 94-118

Research Article

Evaluation of a plastic-degrading bacterium – *Mesobacillus foraminis* SMCD3 for its plant growth promoting activity in *Cicer arietinum* seedlings exposed to polystyrene

Anindita Ghosh Basu[a], Moumita Roy[a], Karishma Tamang[a], Papon Chowhan[b], Rita Som Paul[c], Arka Pratim Chakraborty[b], Swarnendu Roy[a]*

[a]Plant Biochemistry Laboratory, Department of Botany, University of North Bengal, Raja Rammohunpur, Dist. Darjeeling, West Bengal, India
[b]Department of Botany, Raiganj University, Raiganj, Uttar Dinajpur- 733134, West Bengal, India
[c]Department of Botany, Siliguri College, Siliguri, Dist. Darjeeling, West Bengal, India

Abstract

The accumulation of polystyrene (PS) in terrestrial ecosystems poses serious environmental and agricultural concerns, necessitating effective and sustainable bioremediation strategies. In this study, a bacterial isolate, *MesoBacillus foraminis* strain SMCD3, obtained from municipal dumping ground soil, demonstrated significant PS-degrading capability, achieving a 14% reduction in PS weight when cultured in mineral salt medium with PS as the sole carbon source, accompanied by high cell density, indicating efficient metabolic assimilation under nutrient-limited conditions. Enzymatic characterization revealed that PS degradation is primarily mediated through non-classical pathways involving extracellular hydrolases (lipase and esterase) and oxidative enzymes such as alkane hydroxylase and alcohol dehydrogenase. In addition to its biodegradation potential, *MesoBacillus foraminis* strain SMCD3 exhibited multiple plant growth-promoting (PGP) traits, including indole-3-acetic acid production, ammonia generation, and siderophore secretion, suggesting its potential to enhance nutrient availability and phytohormonal regulation. Exposure of *Cicer arietinum* to PS nanoparticles and microplastics significantly inhibited germination, growth, and physiological performance. However, inoculation with *MesoBacillus foraminis* strain SMCD3 effectively mitigated these phytotoxic effects by improving germination parameters, promoting shoot (1.25-2.68-fold) and root (1.00-2.12-fold) elongation, enhancing relative water content (1.01-1.26-fold), and reducing membrane damage (1.60-2.88-fold) compared to PS-MNP-treated seedlings. Moreover, *MesoBacillus foraminis* strain SMCD3 represents a versatile bacterium with dual functional attributes in PS biodegradation and plant growth promotion, underscoring its potential for integrated applications in bioremediation and sustainable agroecosystems under plastic-contaminated conditions.

Keywords: Bioremediation, Ecotoxicology, Microplastics, Nanoplastics, Polystyrene

Article info

Received **12 January 2026**
Revised **21 April 2026**
Accepted **25 April 2026**

DOI: ***https://doi.org/10.55734/nbujps.2025.v17i01.008***

Introduction

Plastic pollution characterizes the Anthropocene as a widespread and enduring contaminant, posing significant ecological, climatic, and human health risks (Bidashimwa et al. 2023; Yan et al. 2024; Gutberlet, 2023). Since the 1950s, global plastic production has exceeded 8.3 billion tonnes, generating approximately 6.3 billion tonnes of waste, which is expected to rise to nearly 12 billion

Correspondence: swarnendubotany@nbu.ac.in

tonnes by 2050, thereby amplifying environmental challenges (Geyer et al. 2017). Plastics are categorized based on their size, source, shape, and chemical composition. According to particle size, they are classified as giant (>1 m), large (<1 m-2.5 cm), medium (<2.5 cm-5 mm), micro (<5 mm-0.1 µm), and nano (<0.1 µm) (Tang et al. 2020). Micro- and nanoplastics (MNPs) are generated from the breakdown of larger plastic materials through various mechanisms such as mechanical abrasion, ultraviolet (UV)-driven photodegradation, chemical oxidation, and microbial biodegradation. These degradation pathways progressively fragment polymers into smaller particles, promoting their persistence, dispersion, and accumulation across terrestrial environments (Duan et al. 2021, Karkanorachaki et al. 2022, Kim et al. 2021, Xiao et al. 2024, Xu et al. 2024). Among various microplastics, including polyethylene (PE), polyethylene terephthalate (PET), and polyvinyl chloride (PVC), polystyrene (PS) has become increasingly prevalent in terrestrial ecosystems owing to its widespread use, persistence, and pronounced ecotoxicological impacts on soil organisms (Muthukumar et al. 2024). In this regard, an investigation around an expanded PS manufacturing site in Minsk, Belarus, revealed widespread soil contamination with PS microplastics (31-8864 particles kg^{-1}), which were detected to a depth of 20 cm in Fluvisols and sediments, indicating vertical migration and surface runoff-mediated transport of raw granules (Kukharchyk and Chernyk, 2022).

Polystyrene (PS) micro- and nanoplastics negatively affect terrestrial biota by impairing plant growth and inducing oxidative and genotoxic stress, and can bioaccumulate through the food chain, posing potential health risks to animals and humans (Ullah et al. 2023). Polystyrene particles impair terrestrial plants across morphological, physiological, biochemical and molecular levels. Growth inhibition, including reduced root length and biomass, is widely reported (Kaur et al. 2022; Li et al. 2020; Dey et al. 2022). PS-MNPs decrease chlorophyll, soluble sugars and antioxidant activity while elevating reactive oxygen species (ROS), hydrogen peroxide (H_2O_2), malondialdehyde (MDA), and proline, indicating oxidative stress (Li et al. 2020; Dey et al. 2022). Cytotoxicity, nuclear abnormalities and micronuclei formation reflect strong genotoxic effects (Kaur et al. 2022). Altered antioxidant enzymes, such as reduced catalase with increased superoxide dismutase (SOD)/peroxidase (POX), further indicate metabolic disruption (Taylor et al. 2022). Polystyrene microplastics (PS-MP) also exert negative effects on *Cicer arietinum*, causing reduced seedling growth, impaired photosynthetic function, and heightened oxidative stress (Dey et al. 2023). Toxicity intensifies with increasing concentration, larger particle size, and unmodified or positively charged surfaces, leading to greater root damage, elevated ROS and MDA accumulation, and altered key antioxidant enzymes (Dey et al. 2023).

Therefore, mitigating the toxic impacts of PS in agroecosystems requires rapid advancement in sustainable degradation approaches. Polystyrene degrades through thermal, oxidative, photochemical, ultrasonic, and chemical pathways. Thermal degradation induces radical chain scission, with pyrolysis yielding up to 85% styrene monomer (Abbas-Abadi, 2021; Marquez et al. 2023). Oxidative and photodegradation involve UV-driven radical formation that can reduce molecular weight and structural integrity (Yusif & Haddad, 2013). Ultrasonic degradation uses cavitation under inert atmospheres to lower polymer molecular mass (Zimmermann et al., 2020). Chemical pathways, particularly pyrolysis and hydro- or steam-assisted depolymerization, convert PS into styrene and hydrocarbon products efficiently (Marquez et al., 2023). Certain microorganisms can initiate oxidative depolymerization of this highly stable aromatic polymer, enabling surface oxidation, chain scission, and limited assimilation previously thought biologically unattainable, further offering a potential eco-friendly biological route for managing plastic pollutants (Mohanan et al. 2020). Bacterial degradation of PS has been reported in several taxa. *Bacillus* spp. and Pseudomonas spp. from plastic dump sites degrade HI-PS within 14 days under controlled incubation (Mohan et al. 2016). Mixed bacterial communities, including Stenotrophomonas maltophilia, *Bacillus* velezensis, and Acinetobacter radioresistens, can significantly reduce PS-MPs mass over 60 days (Xiang et al. 2023). Soil-derived bacteria such as *Pseudomonas aeruginosa*, *Bacillus subtilis*, *Staphylococcus aureus*, and *Streptococcus pyogenes* also demonstrate PS-degrading potential over extended incubation (Asmita et al. 2015).

Interestingly, PS-degrading plant growth-promoting bacteria (PGPB) represent a dual-function biotechnological strategy integrating microplastic biodegradation with soil health enhancement. For instance, *Bacillus spizizenii*, a newly reported PGPB, exhibited 85.86% degradation of PS-MPs within 30 days (Chandel et al. 2025). Concurrent expression of plant growth-promoting traits, including Indole-3-acetic acid (IAA) synthesis, phosphate solubilization, ammonia, hydrogen cyanide (HCN), and siderophore production, demonstrates its

functional stability in the presence of PS. Liu et al. (2023) showed that PE-MP combined with cadmium significantly reduced sorghum growth, while inoculation with *Bacillus* sp. SL-413 decreased ROS accumulation, restored antioxidant balance, and increased biomass by up to 44.6%. Transcriptomic analysis revealed bacterial enhancement of phenylpropanoid, photosynthesis, flavonoid, and MAPK signalling pathways, collectively improving plant stress tolerance and growth under polymer-associated contamination. This dual capability underscores its relevance for sustainable bioremediation in agroecosystems. However, there is a dearth of reports in this connection. Therefore, in view of the environmental persistence of PS and its detrimental effects on crop growth, the present study was undertaken to isolate and characterize PS-degrading soil bacteria and to evaluate their plant growth-promoting (PGP) attributes. We hypothesized that bacterial isolates might possess both polymer-degrading and PGP traits, which could mitigate the adverse effects of polymer contamination on plant growth. Therefore, the dual-functional isolate was assessed for its ability to degrade PS and promote the growth of *Cicer arietinum*, to explore a sustainable strategy for the simultaneous bioremediation of a plastic-contaminated area and enhancement of agricultural health.

Materials and methods

Source of the microorganism

Soil samples were collected from a municipal dumping ground in North Bengal, West Bengal, India. At each site, about 200 g of soil was taken from a depth of 10 cm using pre-sterilized stainless-steel corers to prevent cross-contamination. The samples were placed in sterile, zipper-sealed polyethylene bags labelled with sample identifiers and stored at room temperature until further experiments. For microbial isolation, 1 g of each soil sample was suspended in 10 mL of sterile distilled water to prepare a stock solution, followed by serial tenfold dilutions up to 10^{-10} under aseptic conditions. Aliquots from dilutions 10^{-1} to 10^{-10} were spread on Nutrient Agar (NA) plates using a sterile L-shaped spreader. The plates were incubated at 37 °C for 24 h to allow bacterial growth. Well-isolated colonies were purified by repeated streaking on fresh NA plates until distinct and pure cultures were obtained. Pure isolates were maintained on NA slants at 4 °C for future analysis.

Morphological characterisation of bacterial strains

Gram staining was carried out following the method of Moyes et al. (2009) with minor modifications. Bacterial smears were prepared on clean, grease-free glass slides, air-dried, and heat-fixed. The fixed smears were sequentially stained with crystal violet, treated with Gram's iodine, decolourised with 95% ethanol, and counterstained with safranin, with gentle rinsing between steps. After air drying, the stained preparations were examined under a Carl Zeiss Primovert inverted phase-contrast microscope to determine the morphology of the bacterial isolates.

Screening of bacterial isolates for PS-degrading characteristics

Weight loss assessment

Pre-treatment of PS Films

Expanded polystyrene (PS) sheets were cut, weighing approximately 10 mg, using a sterile blade. The PS were thoroughly washed with sterile distilled water and disinfected with 99.9% (v/v) ethanol. Subsequently, the PS films were air-dried under aseptic conditions in a laminar airflow cabinet until completely dry.

In Vitro biodegradation assay of pre-treated polystyrene films

The biodegradation potential of bacterial isolates was evaluated by following the method described by Chaudhary et al. (2021) where pre-treated PS in a Mineral Salt Medium containing ferrous sulfate ($FeSO_4$, 0.001 g/L), calcium chloride dihydrate ($CaCl_2 \cdot 2H_2O$, 0.002 g/L), magnesium sulfate heptahydrate ($MgSO_4 \cdot 7H_2O$, 0.02 g/L), potassium dihydrogen phosphate (KH_2PO_4, 0.04 g/L), sodium chloride (NaCl, 0.1 g/L), ammonium sulfate ($(NH_4)_2SO_4$, 0.2 g/L), and dipotassium hydrogen phosphate (K_2HPO_4, 0.5 g/L), adjusted to pH 7.0. Sterile culture tubes containing 10 mL of MSM were supplemented with 10 mg of PS. Test sets were inoculated with bacterial cultures, while uninoculated and bacteria-only controls were maintained. After six weeks, bacterial growth was measured at 600 nm (OD_{600}), and residual PS films were washed with ethanol and sterile distilled water, dried at 50 °C for 2 h, and weighed to assess degradation.

Polystyrene-degradation related biochemical tests of SMCD3

Alkane hydroxylase activity

Alkane hydroxylase activity was evaluated using a slightly modified vapour-phase alkane plate assay with diesel oil as the carbon source, following the method of Kloos et al. (2007). Minimal Salt Medium (MNSM) composed of NH_4Cl (1 g/L), $MgSO_4 \cdot 7H_2O$ (0.2 g/L), $CaCl_2$ (0.05 g/L), K_2HPO_4 (1.5 g/L), KH_2PO_4 (0.5 g/L), and agar (15 g/L) was prepared without a carbon source. The bacterial isolate was spot-inoculated, and a sterile Whatman filter paper disc attached to the Petri dish lid was loaded with 150 µL diesel oil, sealed with parafilm, and incubated at 30 °C for 3-7 days. Bacterial growth and the presence of milky halos or emulsification zones indicated diesel utilisation and alkane hydroxylase enzyme activity.

Alcohol dehydrogenase (Adh) activity

Alcohol dehydrogenase (Adh) activity was assessed using a TTC-based colourimetric plate assay. Minimal Salt Medium (MNSM) agar supplemented with 0.5 % ethanol and 0.05% (w/v) TTC (added at approximately 50°C) was poured into Petri dishes. The bacterial strain was inoculated and incubated for 24-48 hours. The appearance of red-coloured colonies or halos indicated Adh activity, while no colour change suggested the absence of the enzyme (Bochner and Savageau, 1977).

Aromatic ring hydroxylase activity

Aromatic ring hydroxylase activity was qualitatively assessed using a modified ferric chloride ($FeCl_3$) assay with toluene vapour as the substrate, following the method of Fuchs et al. (2011). The bacterial isolate was spot-inoculated onto carbon-free Minimal Salt Medium (MNSM) agar plates and exposed to toluene vapour via filter paper discs fixed to the Petri dish lids. After incubation, plates were flooded with 1% (w/v) $FeCl_3$. The appearance of halos around colonies indicated catechol formation, confirming aromatic ring hydroxylase activity.

Aromatic ring-cleaving dioxygenase activity

Aromatic ring-cleaving dioxygenase activity was qualitatively assessed on catechol-enriched, slightly modified MNSM agar plates following Nahar (1994). The MNSM was supplemented with 0.5% catechol as the sole carbon source, and the bacterial isolate was inoculated and incubated at 30 °C for 24-48 h. The formation of yellow halos or pigmentation around colonies indicated catechol oxidation via dioxygenase-mediated aromatic ring cleavage, confirming enzyme activity.

Esterase activity

Esterase activity of bacterial isolates was qualitatively evaluated using Tween 80 agar medium following the method of Aktas et al. (2002). The bacterial isolate was inoculated onto the plates and incubated at 30 °C for 10 days. The formation of white precipitates or opaque halos surrounding the colonies indicated positive esterase activity, whereas the absence of such zones denoted a negative reaction.

Laccase production

Laccase production was qualitatively assessed following Minhas et al. (2024) with slight modifications. The bacterial isolate was grown in nutrient broth containing 0.5 mM filter-sterilised guaiacol and incubated at 30 °C for up to 10 days under shaking (150-200 rpm). The appearance of reddish-brown colouration in the broth, due to guaiacol oxidation, indicated positive laccase activity, while no colour changes denoted negative results.

Biochemical characterisation of SMCD3

Catalase activity

The catalase activity of the bacterial isolate was determined using the glass slide method as described by Khatoon et al. (2022). A freshly grown bacterial colony was placed on a clean glass slide, followed by the addition of a drop of 3% hydrogen peroxide (H_2O_2). The rapid formation of oxygen bubbles indicated a positive catalase reaction, confirming the enzymatic breakdown of H_2O_2 into water and oxygen.

Citrate utilization

Citrate utilization by yeast was evaluated using Simmons' Citrate Agar (SCA) as the sole carbon source (Khodadadi et al. 2025). The medium was aseptically inoculated and incubated at 30-37 °C for 24-48 h. A positive result was indicated by growth accompanied by a colour change from green to blue, reflecting alkaline byproducts of citrate metabolism, whereas no colour change indicated a negative reaction.

Cellulase activity

Cellulase activity was qualitatively evaluated following Toghueo et al. (2017) using glucose-yeast extract-peptone (GYP) agar supplemented with 0.5% (w/v) sodium carboxymethyl cellulose (CMC). The bacterial isolate was spot-inoculated and

incubated at 37 °C for 5-6 days. Plates were stained with 0.2% (w/v) Congo Red and destained with 1 M NaCl. The formation of clear or pale-yellow halos around colonies indicated cellulase-mediated hydrolysis of CMC.

Urease activity

Urease activity was qualitatively determined using Christensen's urea agar following the method explained by Christensen (1946). The bacterial isolate was spot-inoculated and incubated at 30 °C for 3-5 days. Urease-positive cultures hydrolysed urea to ammonia (NH_3) and carbon dioxide (CO_2), increasing the pH and turning the phenol red indicator from yellow to pink, while no colour change indicated a negative result.

Gelatinase activity

Gelatinase activity was detected using a nutrient gelatin medium. The medium was autoclaved, and bacterial culture was stab-inoculated into the gel and incubated at 37 °C for up to 7 days. Tubes were examined daily for liquefaction. To confirm hydrolysis, tubes were chilled at 4 °C for 30 minutes. Persistent liquefaction after cooling indicated positive gelatinase activity, while re-solidification denoted a negative result (Cruz et al. 2012).

Lipase activity

Lipase activity was qualitatively assessed using a Tween 20-supplemented peptone agar medium by following the method described by Salihu et al. (2011). The bacterial strain was spot-inoculated and incubated at 37 °C for 24-48 hours. Lipase activity was indicated by the formation of a clear or opaque halo around colonies due to the hydrolysis of Tween 20.

Carbohydrate fermentation of glucose, fructose, and galactose

Carbohydrate fermentation was performed according to the American Society for Microbiology (Reiner, 2012). Phenol red broth (pH 7.4 ± 0.2) was prepared containing peptone (10 g/L) and NaCl (5 g/L), with 1% glucose, fructose, or galactose as the sole carbon source. The medium, dispensed with inverted Durham tubes, was sterilized at 120 °C for 15 min. The test isolate was aseptically inoculated and incubated at 35-37 °C for 24 h under static conditions. Acid production was indicated by a colour shift from red to yellow, while trapped bubbles confirmed gas formation.

Plant growth-promoting activities

Indole-3-acetic acid (IAA) production

Indole-3-acetic acid (IAA) production was quantitatively assessed using Salkowski reagent, prepared by combining ferric chloride and perchloric acid. The isolate was cultured in Luria-Bertani (LB) broth, and the cultures were centrifuged at 12,000 rpm for 10 min at 4 °C to obtain cell-free culture supernatant (CFCS). The CFCS was mixed with Salkowski reagent in a 1:1 ratio and incubated at 37°C for 1 hour in the dark. The development of a pink to reddish colouration was considered indicative of IAA production (Srinivasan et al. 2025).

Indole-3-acetic acid (IAA) utilization

The bacterial isolate was tested for IAA utilization following the protocol described by Leveau and Lindow (2005). Minimal Salt Medium agar containing 0.1-0.5 mM sterile IAA was spot-inoculated with bacterial suspensions and incubated at 30 °C for 24-72 h. Visible growth indicated IAA tolerance or metabolism; absence of growth indicated non-utilization. Uninoculated plates served as controls.

Hydrogen cyanide (HCN) production

Hydrogen cyanide (HCN) production was evaluated following Alström and Burns (1989), in which 100 µL of bacterial culture was streaked on NA supplemented with 4.4 g/L glycine. A Whatman No. 1 filter paper soaked in alkaline picrate solution (2% sodium carbonate in 0.5% picric acid) was placed in the plate lid. Plates were sealed and incubated at 28 °C for 4 days. A colour change from yellow to brown/reddish-brown indicated HCN production (Alström and Burns, 1989).

Protease production

Protease production was assessed using skimmed milk agar (SMA). A 10% (w/v) skimmed milk solution was sterilized at 115 °C for 10 min, while agar was autoclaved separately at 121 °C for 20 min. The solutions were mixed to obtain a final concentration of 1% skimmed milk and poured into Petri plates. The bacterial isolate was spot-inoculated and incubated at 30 °C for 72 h. The formation of a clear zone around colonies was considered indicative of protease activity (Abdelmoteleb et al. 2017).

Ammonia production

Ammonia production was determined by inoculating a 24 h-old bacterial culture into 10 mL peptone

broth, followed by incubation at 37 °C for 48 hours. Post-incubation, 0.2 mL of freshly prepared Nessler's reagent was added, and the development of yellow to brown colouration was considered indicative of ammonia production (Bhatt et al. 2015).

Phosphate-solubilising activity

The primary phosphate-solubilising activity of bacteria was assessed using Pikovskaya's agar medium. Plates were incubated at 37 °C for 7-10 days, and phosphate solubilization was indicated by the formation of a clear halo zone surrounding the bacterial colony (Pikovskaya, 1948).

Amylase activity

The bacterial isolate was aseptically inoculated onto starch agar plates composed of peptone, beef extract, soluble starch, and agar for amylase activity. Cultures were incubated aerobically at 35-37 °C for 24-48 hours. Following incubation, plates were flooded with Gram's iodine solution to detect residual starch (Lal and Cheeptha, 2012).

Siderophore production

Siderophore production by bacterial isolate was assessed using Chrome Azurol S (CAS) agar following the method of Schwyn and Neilands (1987). The bacterial isolate was spot-inoculated and incubated at 28-30 °C for 10-15 days. The development of an orange or yellow halo around colonies indicated siderophore production.

Identification of the most potent plant growth-promoting PS-degrading bacteria

Genomic DNA of the bacterial isolate SMCD3 was extracted using the Quick-DNA™ Fungal/Bacterial Miniprep Kit (Cat. No. D6005, Zymo Research, USA) according to the manufacturer's protocol. The 16S rRNA gene was amplified by PCR using universal primers 27F (5′-GAGTTTGATCATGGCTCAG-3′) and 1492R (5′-TACGGTTACCTTGTTACGACTT-3′). PCR products were visualized on a 1.5% agarose gel and purified for sequencing. The obtained sequences were analyzed using the NCBI GenBank 'nr' database via BLASTn to determine sequence similarity with known bacterial taxa. The phylogenetic tree was constructed using the Neighbour-Joining method, with evolutionary distances calculated by the Kimura 2-parameter model. The analysis included 20 nucleotide sequences, with ambiguous positions removed using pairwise deletion, resulting in 1458 final positions. Analyses were performed using MEGA11.

Growth pattern

Pure bacterial isolates (SMCD3) were cultured overnight in nutrient broth and standardized to approximately 1% (v/v) inoculum. Subsequently, 1 mL of culture was aseptically inoculated into 100 mL sterile nutrient broth (pH 7.0 ± 0.2) in 250 mL Erlenmeyer flasks, following the growth curve methodology described by Maneesha and Subathra (2026). The culture was incubated at 35°C with continuous shaking at 120 rpm to ensure adequate aeration. Growth was monitored at optimized, non-uniform intervals (0-72 h), and optical density (OD_{600}) was measured spectrophotometrically. Growth phases were determined by plotting OD_{600} against time, enabling characterization of lag, exponential, stationary, and decline phases.

Preparation of polystyrene micro-nano-plastics particles (PS-MNPs)

Expanded polystyrene (EPS) was utilized for the preparation of polystyrene micro- and nanoplastic particles (PS-MNP) using the ice-block method described by Kwak and An (2020), with slight modifications. Commercial EPS sheets were procured from a certified local supplier and processed to obtain three defined size fractions: PS nanoparticles (PS-NP; <1 µm), PS microplastics type 1 (PS-MP1; 1 µm-1 mm), and PS microplastics type 2 (PS-MP2; 1-5 mm). EPS fragments were suspended in distilled water and subjected to cryogenic pre-treatment at -20 °C to induce brittleness and facilitate size reduction. The frozen EPS-water composites were mechanically ground using a precision grinder under standardized durations of 20, 10, and 5 minutes for PS-NP, PS-MP1, and PS-MP2, respectively. The resulting suspensions were sequentially sieved to ensure particle size homogeneity and oven-dried to remove residual moisture. To enhance nanoscale uniformity, the PS-NP fraction underwent an additional 5-minute regrinding step, while PS-MP1 and PS-MP2 fractions were vortexed for 2 and 1 minute, respectively, to achieve homogeneous dispersion before experimental applications.

Plant sample and experimental design

The certified seeds of *Cicer arietinum* cv. Kanchan were obtained from the New Bharat Laxmi Nursery, Ghatal, of West Bengal. Seeds with >90 % viability were surface-sterilized using 0.1 % (v/v) sodium hypochlorite for 2 min, followed by triple rinses with sterile double-distilled water. For inoculated treatments, seeds were incubated for 8 h in a suspension of the most efficient PS-degrading bacterial isolate under gentle agitation, then

aseptically air-dried. Uninoculated seeds were also incubated in sterile distilled water for 8 hours. Ten seeds were evenly distributed on each Petri plate to ensure uniform spacing and minimize inter-seed competition.

Seedlings of *Cicer arietinum* L. (chickpea) were cultivated under controlled laboratory conditions to elucidate the influence of PS-MNPs on early plant growth and development. Growth conditions were maintained at 25 ± 2 °C, 55 ± 2 % relative humidity, and a 16 h light/8 h dark photoperiod. A total of 24 sterile Petri plates (10 cm diameter), each lined with a double layer of sterile cotton, served as a uniform, inert, and moisture-retentive growth substrate. Polystyrene particles were applied between the cotton layers at a concentration of 2.4 mg cm^{-2}, representing three size categories: PS-NP, PS-MP1, and PS-MP2. Each set was irrigated with 0.1× Hoagland's nutrient solution to maintain optimal moisture and nutrient availability.

The experiment comprised eight distinct treatment combinations, including two controls, uninoculated and inoculated (both without plastic exposure), and six treatments involving different sizes of polystyrene particles, either with or without bacterial inoculation. Specifically, the treatments were: uninoculated control (no plastic), inoculated control (no plastic), PS-NP (uninoculated), PS-NP (inoculated), PS-MP1 (uninoculated), PS-MP1 (inoculated), PS-MP2 (uninoculated), and PS-MP2 (inoculated). Each treatment was replicated three times, yielding 24 experimental units arranged in a completely randomized design (CRD) to minimize experimental error (Figure 1).

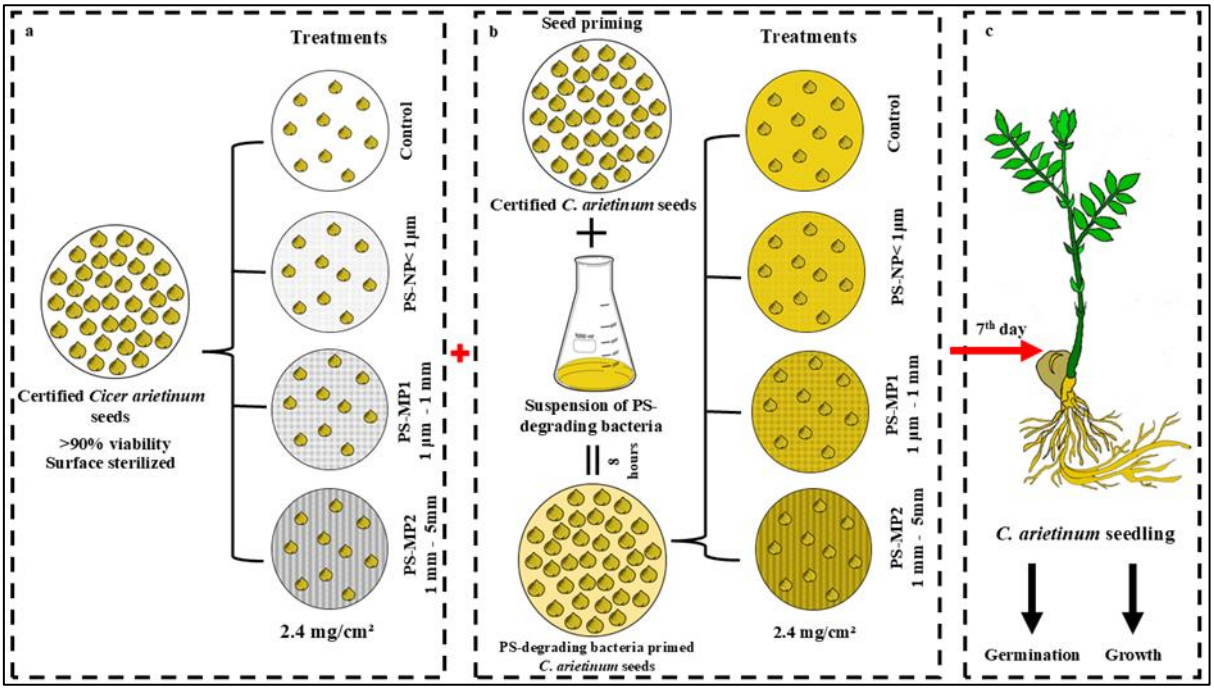

Figure 1. Experimental design for the study of PS-degrading bacteria on plant growth and mitigation of PS stress.

Plant growth promotion, seed germination, and seedling morphological parameters

Germination parameters

Germination percentage (GP) was determined by following the method described by Ullah et al. (2022).

$$GP\ (\%) = \frac{Final\ number\ of\ seeds\ germinated}{Total\ number\ of\ seeds} \times 100$$

Germination energy (GE) was determined according to the formula described by Wang et al. (2021).

$$GE\ (\%) = \frac{N3d}{Nt} \times 100$$

where Nt was the total number of tested seeds, and N3d was the number of seeds on day three.

Mean germination time (MGT) was calculated using the formula:

$$MGT = \frac{\sum dn}{N}$$

where n is the number of seeds germinated on each day, d is the number of days from the start of the test, and N is the total number of seeds germinated at the end of the experiment (Kulkarni et al. 2007).

The coefficient of velocity of germination (CVG) was calculated using the formula described by Aboryia et al. (2024):

$$CVG = \frac{(N_1 + N_2 + \cdots + N_i)}{(N_1T_1 + N_2T_2 + \cdots + N_iT_i)} \times 100$$

where N is the number of seeds germinated on each day, and T is the number of days from sowing corresponding to N.

Morphological parameters

Shoot and root lengths were measured from ten randomly selected seedlings per treatment of three replicates, and the mean values were calculated.

Leaf surface area was measured manually using the graph paper method as described by Sharma et al. (1986).

$$Area\ (mm^2) = Length(mm) \times Width\ (mm)$$

Physiological parameters

Relative water content (RWC) was determined following the method of Barr and Weatherley (1962). Seedlings from each treatment and control were weighed to obtain fresh weight (FW), then immersed in distilled water for 4 hours to reach full turgidity. After removing surface moisture, the turgid weight (TW) was recorded. Samples were then oven-dried at 80 °C for 24 h and weighed to obtain dry weight (DW). RWC was calculated using the formula:

$$RWC = \frac{TW - DW}{FW - DW} \times 100$$

Electrolyte leakage was assessed following the method described by Lutts et al. (1996). Seedlings were rinsed with deionized water and incubated in 10 mL deionized water at 25 °C on a rotary shaker for 24 hours. The initial conductivity (Lt) was measured using a conductivity meter. Samples were then autoclaved at 120 °C for 20 minutes, cooled to room temperature, and the final conductivity (L0) was recorded and calculated using the formula:

$$EL = \frac{L_t}{L_0} \times 100$$

Statistical analysis

All experiments were conducted using three independent biological replicates (N = 3), except for measurements of shoot length, root length, and leaf surface area, which were performed with six replicates (N = 6). Data are presented as mean ± standard deviation (SD). Statistical analyses were carried out using IBM SPSS Statistics 26. Differences among treatment groups were evaluated using one-way analysis of variance (ANOVA), followed by Duncan's multiple range test for post hoc comparisons. Statistical significance was established at a threshold of $p < 0.05$.

Results and discussion

Isolation of soil bacteria from the dumping ground

A total of three distinct bacterial isolates were obtained from soil samples collected from the municipal dumping ground. From the site, three pure bacterial cultures were successfully isolated and designated as SMCD1, SMCD2, and SMCD3. All isolates were purified by repeated streaking on nutrient agar plates under aseptic conditions and maintained for further characterization (Figure 2).

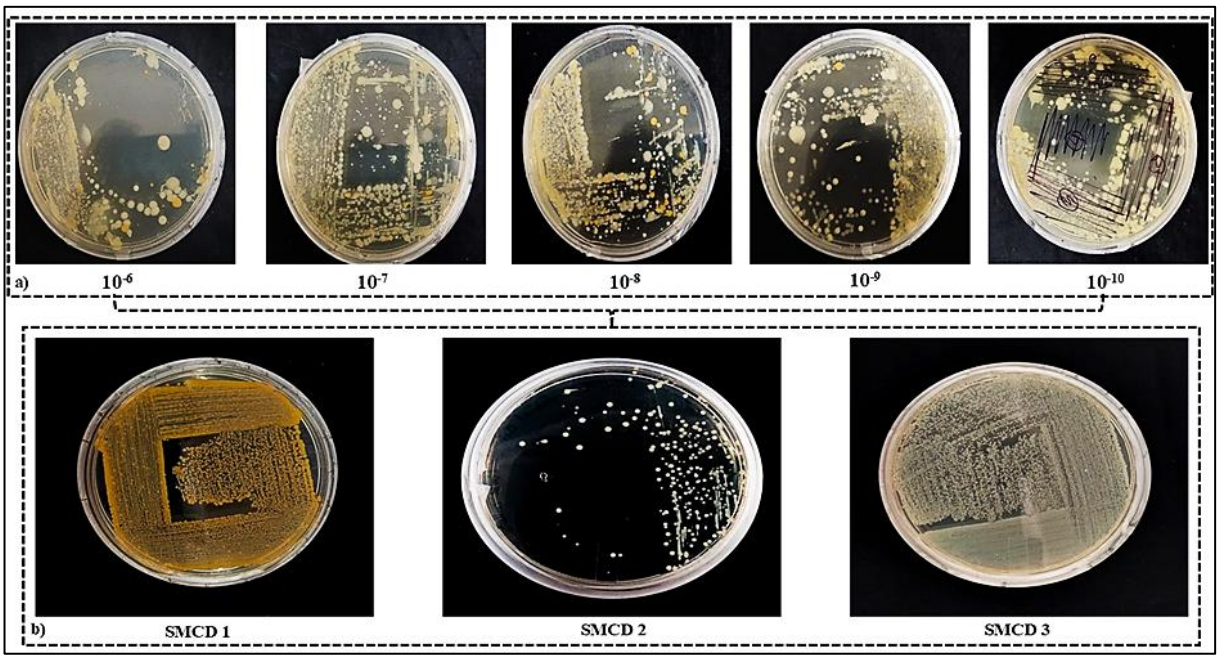

Figure 2. Isolation of bacterial pure culture by serial dilution collected from the Municipal Corporation Dumping Ground. a) serial dilution for the isolation of bacteria, b) pure culture of the selected bacterial strains.

Characterization of the bacterial isolates for PS-degradation

After 6 weeks of incubation in a mineral salt medium (MSM) containing PS as the sole carbon source, the degradation efficiency was observed among the three bacterial isolates (Figure 3). SMCD3 exhibited the highest polystyrene degradation, achieving a 14% reduction in polymer weight, indicative of potent metabolic or enzymatic breakdown activity. SMCD1 followed closely with 13% weight loss, reflecting comparable degradation potential. In contrast, SMCD2 induced only 7% weight reduction, suggesting a relatively lower capacity for PS depolymerisation under nutrient-limited conditions (Figure 3). Bacterial proliferation was concurrently assessed after 6 weeks of incubation to evaluate metabolic activity in response to polystyrene utilisation. SMCD3 showed the highest cell density (2.45×10^8 cells/mL), correlating with its superior degradation capability and suggesting efficient utilisation of polystyrene degradation products for growth. SMCD2 reached a moderate cell density (6.64×10^7 cells/mL), consistent with its intermediate degradative performance. Notably, SMCD1 displayed a markedly low cell density (1.6×10^6 cells/mL) despite high weight loss, implying a degradation mechanism primarily mediated by extracellular enzymes or biofilm-associated activity rather than extensive planktonic growth (Figure 3).

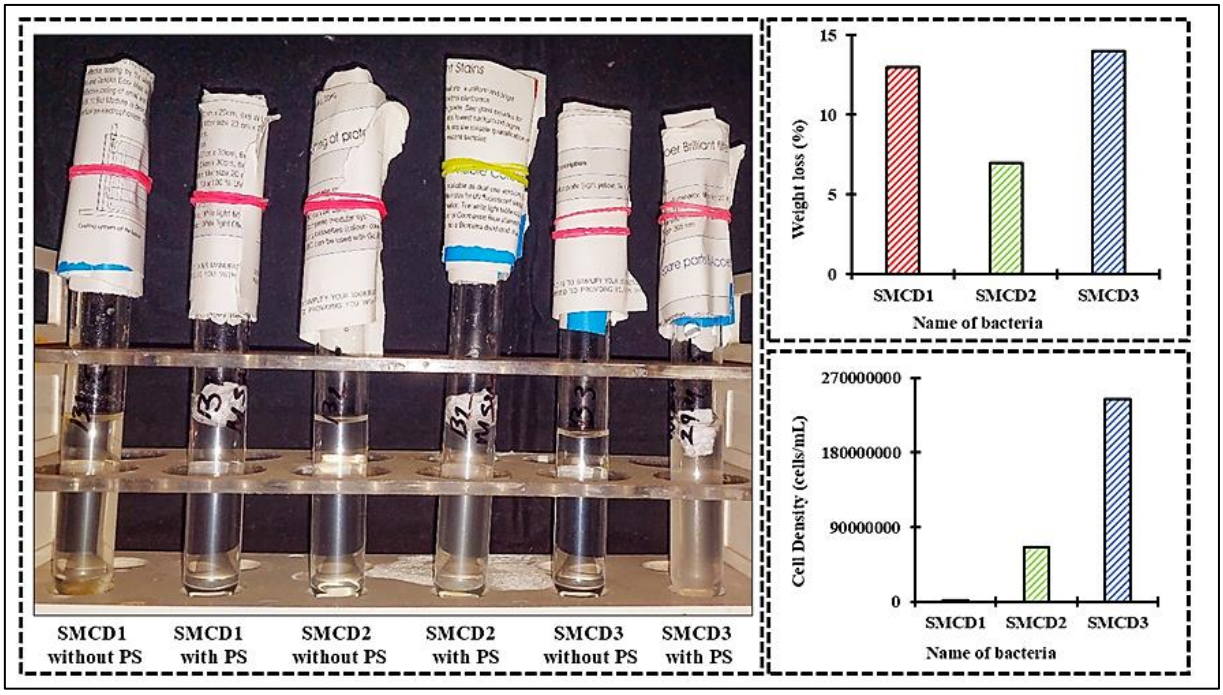

Figure 3. Weight loss (%) of PS and cell density (cells/mL) in mineral salt media inoculated with bacteria

Therefore, this study validated the PS degradation potential of bacterial isolates (SMCD1, SMCD2, and SMCD3) obtained from a dumping ground, which could utilize PS as the sole carbon source. The observed results are in strong agreement with the findings of Ugueri et al. (2022), who similarly demonstrated that *Bacillus subtilis* and *Pseudomonas aeruginosa* isolated from plastic-contaminated soils effectively degraded PS under nutrient-limited conditions (Ugueri et al. 2022). Among the isolates, SMCD3 exhibited the highest PS degradation efficiency, showing a 14% reduction in polymer weight and a cell density of 2.45×10^8 cells/mL. This suggests strong metabolic activity and efficient assimilation of PS breakdown products, consistent with the behaviour of *Bacillus subtilis*, which demonstrated similar outcomes in Ugueri et al.'s study. The ability of these bacteria to utilise PS as a sole carbon and energy source underlines their enzymatic adaptability in oligotrophic environments. SMCD1, despite showing comparable weight loss (13%), had a significantly lower cell density (1.6×10^6 cells/mL). This discrepancy suggests that PS degradation may have occurred predominantly via extracellular enzymatic action or biofilm-mediated surface oxidation, a mechanism attributed to *Pseudomonas aeruginosa* in prior research. SMCD2 presented moderate degradation (7%) and cell density (6.64×10^7 cells/mL), indicating partial utilisation of PS. The distinct degradation efficiencies observed across the isolates reflect species-specific enzymatic capabilities and adaptive responses to carbon limitation. These findings reaffirm that soil-dwelling microbes from dump environments, when

challenged with PS as the sole carbon source, can initiate measurable biodegradation processes.

Morphological characterisation of SMCD3

Among the three isolates, the most potent PS-degrading bacterium, i.e. SMCD3, exhibited purple-coloured cells after Gram staining, confirming it as a Gram-positive bacterium. Moreover, SMCD3 showed numerous small, densely packed cocci with uniform staining (Figure 4a). This structural feature indicates a thick peptidoglycan layer, commonly associated with *Bacillus* and related genera, which are frequently reported as potent polyethylene plastic degraders, and moreover often more resistant to environmental stress and are known to produce diverse extracellular enzymes beneficial for polymer degradation (Yoon et al. 2012).

Polystyrene-degradation related biochemical tests of SMCD3

Alkane hydroxylase activity was qualitatively examined, and SMCD3 exhibited robust bacterial growth, indicating efficient utilisation of hexadecane and confirming the expression of alkane hydroxylase enzyme pathways (Figure 4b). The control plate remained clear without any microbial growth. This result suggests that SMCD3 harbours functional alkane hydroxylases essential for initiating hydrocarbon degradation via terminal oxidation pathways (Figure 4b). This aligns with Hou and Majumder (2021), who identified alkane hydroxylases as key enzymes in PS depolymerisation by cleaving C-C bonds (Hou & Majumder, 2021). More interestingly, alcohol dehydrogenase (ADH) activity was detected in SMCD3, as evidenced by the development of a red-coloured zone upon TTC application, which turns into insoluble triphenyl formazan (TPF) by reducing equivalents generated during ethanol metabolism, indicating alcohol dehydrogenase activity (Figure 4c). This finding indicates NAD^+-dependent oxidation of ethanol to acetaldehyde. The presence of ADH suggests oxidative metabolic pathways in SMCD3, which could be involved in PS degradation by breaking down hydroxylated intermediates (Urbanek et al. 2020). This enzyme may play a role in catabolizing styrene monomers or oligomers derived from PS breakdown. The aromatic ring hydroxylase activity of PS-degrading bacterial isolates was evaluated to determine their ability to initiate aromatic compound oxidation. In the assay, SMCD3 exhibited no growth or colour change, suggesting a lack of hydroxylase activity under the tested conditions (Table 1). This is consistent with literature indicating that, although aromatic ring hydroxylases may contribute to PS degradation, they play only a secondary role and are not universally present or active in all degrading microorganisms, which may instead rely on alternative oxidative enzymes (Hou and Majumder, 2021). The isolate indicates a negative result for aromatic ring-cleaving dioxygenase activity in the strain under the experimental conditions (Table 1). The absence of detectable catechol dioxygenase activity suggests that the isolate does not employ the classical catechol-mediated ortho- or meta-cleavage pathways. This is in agreement with reports on *Exiguobacterium* spp., which indicate the presence of atypical aromatic ring-cleaving dioxygenases that catalyze ring degradation via alternative oxygen-dependent mechanisms independent of catechol intermediates (Parthasarathy et al. 2022). Moreover, esterase activity was observed in SMCD3. A distinct, milky-white opaque zone was formed around the bacterial growth, indicating hydrolysis of Tween 80 and subsequent calcium salt precipitation. The esterase-positive result in SMCD3 indicates its enzymatic capacity to cleave ester bonds, potentially contributing to PS degradation by initiating surface-level structural modifications (Figure 4e). Our results are in accordance with previous studies by other researchers, who also reported that the enzyme esterase hydrolyses ester bonds and is important in initiating plastic degradation (Wilkes & Aristilde, 2017). The absence of laccase activity in the present study implies that PS degradation by these isolates likely proceeds through non-oxidative enzymatic pathways, such as those involving hydrolases (Table 1).

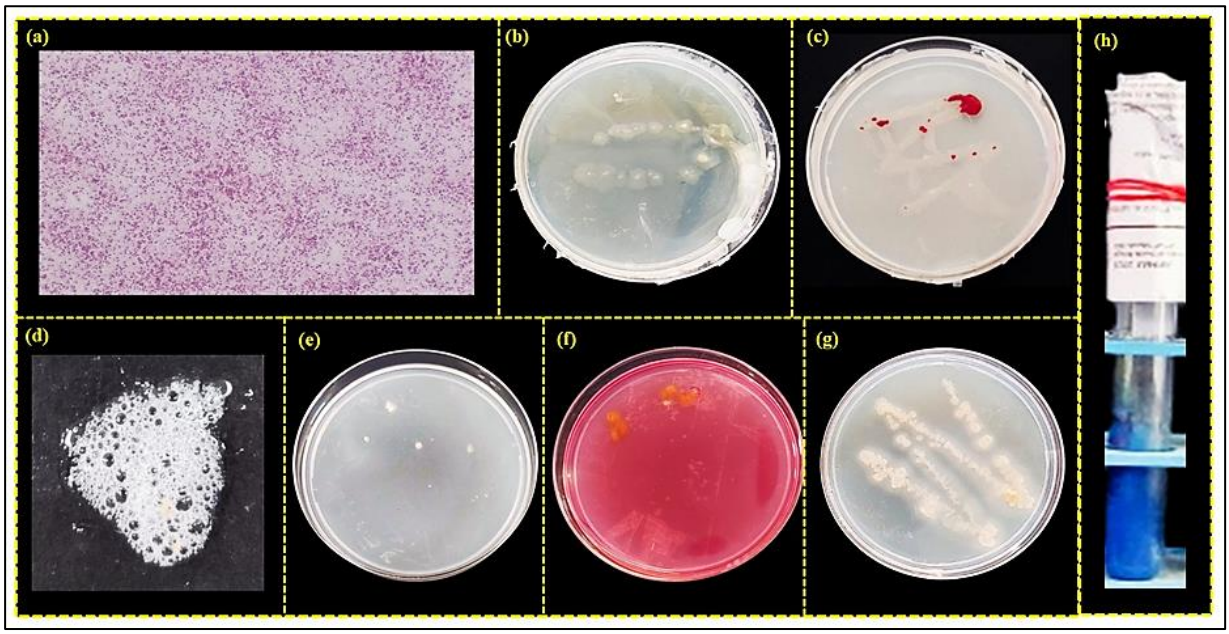

Figure 4. (a) Gram staining, (b) Alkane hydroxylase activity, (c) Alcohol dehydrogenase activity, (d) Catalase activity, (e) Esterase activity, (f) Cellulase activity, (g) Lipase activity, and (h) Citrate utilization of the most potent PS-degrading bacteria

Biochemical characterisation of SMCD3

In the case of the citrate utilization test, SMCD3 showed a positive result (Figure 4h), and according to another study by Özdemir et al. (2022), two Gram-positive and thermophilic bacteria, *AnoxyBacillus flavithermus* ST3 and Anoxy*Bacillus* sp. ST6 can effectively degrade polyethylene microparticles. More interestingly, besides their polymer bioremediation capability, both of these strains not only produce alpha-Amylase but are also able to utilize citrate as a source of energy. Catalase activity was also detected in SMCD3. Upon exposure to 3% hydrogen peroxide, immediate and intense bubble formation was observed on SMCD3 (Figure 4d). Researchers reported that catalase is a crucial enzyme during oxidative stress, and its presence in SMCD3 supports and suggests that they can survive oxidative stress conditions during PS degradation, which often generates reactive oxygen species (ROS) (Restrepo-Flórez et al. 2014). Cellulase activity was assessed to determine the ability of the PS-degrading bacterial isolate to hydrolyse cellulose, which reflects its extracellular enzyme potential. SMCD3 exhibited visible zones of clearance around the bacterial growth when inoculated on carboxymethyl cellulose (CMC) agar and subsequently stained with Congo red. The appearance of clear halos against the red background confirmed cellulase-mediated hydrolysis of cellulose, indicating positive cellulolytic activity. The cellulase activity in SMCD3 suggests its ability to degrade plant-based polysaccharides, which may enhance biofilm formation on plastic surfaces and contribute indirectly to PS-degradation (Figure 4f). This supports findings by Šaraba et al. (2023), who showed that some environmental bacteria can use cellulases to survive in low-nutrient conditions (Šaraba et al. 2023). Urease activity was assessed using Christensen's urea agar medium, where a positive result is indicated by a pink colour change due to ammonia release and subsequent pH increase. SMCD3 exhibited no detectable urease activity in the PS-degrading bacterial isolate under the tested conditions (Table 1). In contrast, *Bacillus* strains isolated by Oyewusi et al. (2020) showed urease positivity alongside pollutant degradation, but their degradative enzymes targeted halogenated organics, not synthetic polymers like PS (Oyewusi et al. 2020). Thus, urease appears non-essential for PS biodegradation in the case of SMCD3. The tested isolate, SMCD3, also showed the absence of laccase activity, as well as the absence of guaiacol oxidation in the assay medium (Table 1). In contrast, previous studies have identified several soil-derived bacterial strains capable of producing laccase, which contributed to plastic degradation through oxidative depolymerisation of phenolic substrates (Abirami et al. 2021). The gelatinase activity assay revealed no hydrolysis of gelatin in the tested PS-degrading bacterial strain, where SMCD3 showed solidified media after refrigeration, similar to the negative control, indicating the absence of gelatinase production (Table 1). This aligns with findings by Tan et al. (2022), where *Bacillus* megaterium expressed extracellular PS-degrading enzymes such as lipases, esterases, and cutinase-hydrolase not

involved in gelatin hydrolysis (Tan et al. 2022). The absence of gelatinase activity further confirms that PS degradation by these isolates does not rely on proteolytic enzymes, but instead on specific hydrolases targeting synthetic polymers. Lipase production was assessed using tributyrin agar, where lipase-positive colonies hydrolyse tributyrin, forming a clear halo around the bacterial growth. SMCD3 exhibited a prominent and well-defined zone of clearance, indicating substantial lipase activity. This suggests that SMCD3 can secrete extracellular lipases that hydrolyse lipid substrates. The uninoculated control plate remained clear and lacked any halo formation. Thus, the result clearly distinguishes SMCD3 as the lipolytic strain among the isolates, potentially contributing to PS degradation via ester bond cleavage in polymeric contaminants (Figure 4g). This enzymatic trait is consistent with findings by Tan et al. (2022), who identified extracellular PS-degrading enzymes, including lipases and esterases, from *Bacillus* megaterium, with molecular weights between 20 and 60 kDa, contributing to PS depolymerisation via hydrolysis of ester bonds (Tan et al. 2022). No carbohydrate fermentation was observed in isolate SMCD3 for glucose, fructose, and galactose, as indicated by the absence of colour change in phenol red broth and gas production in Durham tubes under the tested conditions (Table 1). This suggests that the isolate may rely on oxidative metabolism rather than fermentation for energy production. Importantly, this does not contradict its potential for PS degradation, as PS is a non-carbohydrate, hydrophobic polymer that is degraded through oxidative enzymatic mechanisms involving monooxygenases, cytochrome P450, and related enzymes (Hou and Majumder, 2021).

Plant growth-promoting attributes of SMCD3

SMCD3 exhibited a strong orange to brown colouration, confirming the release of ammonia. The intensity of the developed colour suggests that SMCD3 showed relatively higher ammonia production (Figure 5b). This result affirms the ability of this PS-degrading bacterium to participate in nitrogen metabolism, indicating its potential role as a plant growth-promoting bacterium (PGP). Interestingly, ammonia production is a significant plant growth-promoting trait that enhances nitrogen availability in the rhizosphere, thereby supporting plant nutrient uptake and growth (Bhattacharyya & Jha, 2012). Phosphate solubilization in bacteria is primarily mediated by the secretion of organic acids that acidify the environment and release bound phosphate (Timofeeva et al. 2023), but in our study, phosphate solubilization activity was absent in isolate SMCD3, as evidenced by the lack of halo zone formation on phosphate solubilization medium (Table 1). This indicates that the isolate is unable to solubilize insoluble phosphate under the tested experimental conditions. Proteases play a crucial role in the mineralization of organic nitrogen by catalyzing the hydrolysis of complex proteins into simpler peptides and amino acids, thereby contributing to nutrient cycling in the rhizosphere (Afrin et al. 2024). The absence of a clear zone of hydrolysis in isolate SMCD3 indicates a lack of detectable extracellular protease activity under the tested conditions, suggesting that the isolate does not actively secrete proteolytic enzymes involved in protein degradation. Interestingly, SMCD3 tested positive for amylase activity after post-incubation, and iodine staining revealed a clear halo or zone of clearance around the colonies across the starch agar surface (Figure d). This suggests that this bacterium has extracellular amylolytic enzymes under the given assay conditions, and interestingly, researchers proved that amylases are generally produced by bacteria in response to polysaccharide-rich environments and are primarily involved in starch degradation (Rao et al. 1998). Moreover, the positive siderophore production observed in isolate SMCD3, as indicated by the colour change on chrome azurol S (CAS) agar, confirms the secretion of high-affinity Fe^{3+}-chelating compounds under iron-limited conditions (Figure 5e). The CAS assay detects siderophore-mediated removal of iron from the dye complex, resulting in a visible colour shift. Siderophores function as low-molecular-weight secondary metabolites that form stable Fe^{3+}-siderophore complexes, facilitating iron uptake via specific transport systems. Furthermore, siderophore-producing bacteria enhance iron availability in the rhizosphere and contribute to plant growth promotion. They also suppress phytopathogens through competitive iron sequestration, highlighting their dual role in nutrient acquisition and biocontrol (Zhang et al. 2023).

Table 1. Biochemical and plant growth-promoting characteristics of isolate SMCD3. (+) Positive activity; (++) Strong positive activity; (−) Negative activity

Parameters	Tests / Methods	Result
Polystyrene-degradation related tests	Alkane hydroxylase activity	++
	Alcohol dehydrogenase activity	+
	Aromatic ring hydroxylase activity	−
	Aromatic ring cleavage dioxygenase activity	−
	Esterase activity	+
	Laccase activity	−
Biochemical characterization	Citrate utilization	+
	Catalase activity	++
	Cellulase activity	++
	Urease activity	−
	Gelatinase activity	+
	Lipase activity	++
	Glucose fermentation	−
	Galactose fermentation	−
	Fructose fermentation	−
Plant Growth-Promoting Characteristics	IAA synthesis	+
	IAA utilization	−
	HCN production	−
	Protease activity	−
	Ammonia production	+
	Phosphate solubilization	−
	Amylase activity	++
	Siderophore production	+

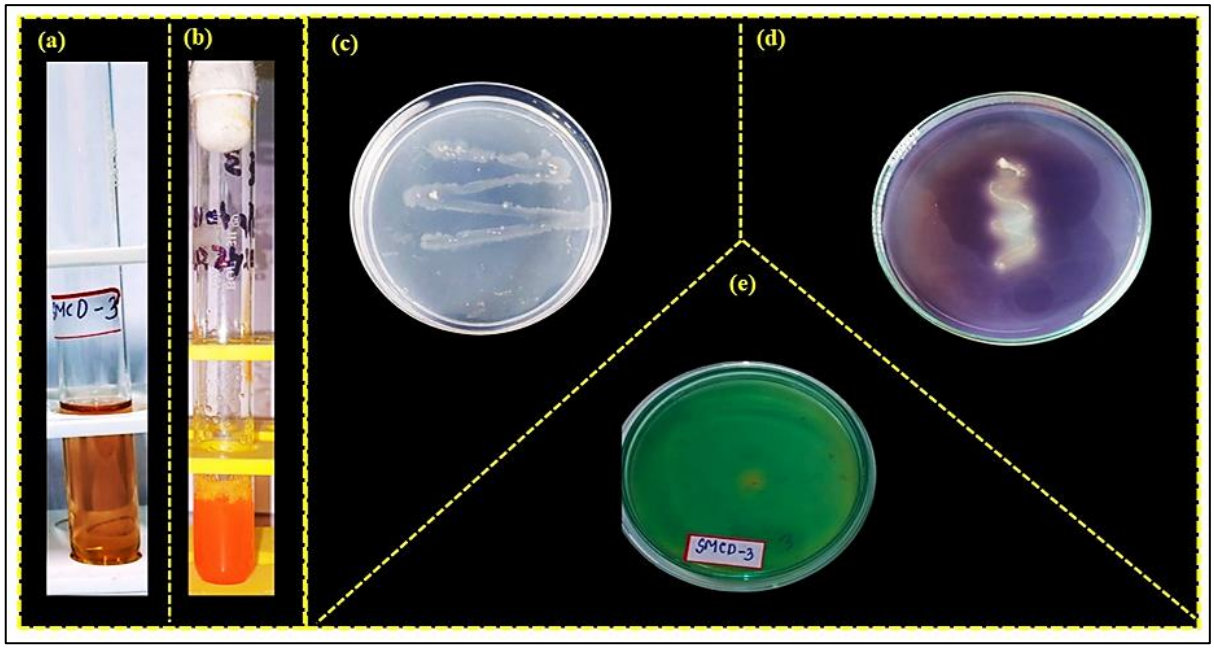

Figure 5. (a) IAA production, (b) Ammonia production, (c) IAA utilization, (d) Amylase production, and (e) Siderophore production of the most potent PS-degrading bacteria

Identification of SMCD3 and study of growth pattern

The taxonomic identification of SMCD3 was established through combined 16S rRNA gene sequencing, database comparison, and phylogenetic analysis. A single discrete amplicon of approximately 1500 bp was obtained, and high-quality bidirectional sequencing generated a 1386 bp consensus sequence. This sequence was deposited in the NCBI GenBank database under accession number PZ235437 as *MesoBacillus foraminis* strain SMCD3. Moreover, BLAST analysis revealed high nucleotide identity (≥98-99%) with complete query coverage against the *MesoBacillus foraminis* reference sequences. Phylogenetic analysis using the Neighbour-Joining method further showed that strain SMCD3 clusters within the *M. foraminis* clade, with very low evolutionary divergence from closely related strains. The consistency between sequence similarity, GenBank annotation, and phylogenetic positioning provides strong and reliable evidence for its classification. Therefore, strain SMCD3 is conclusively identified as *MesoBacillus foraminis* strain SMCD3 (Figure 6).

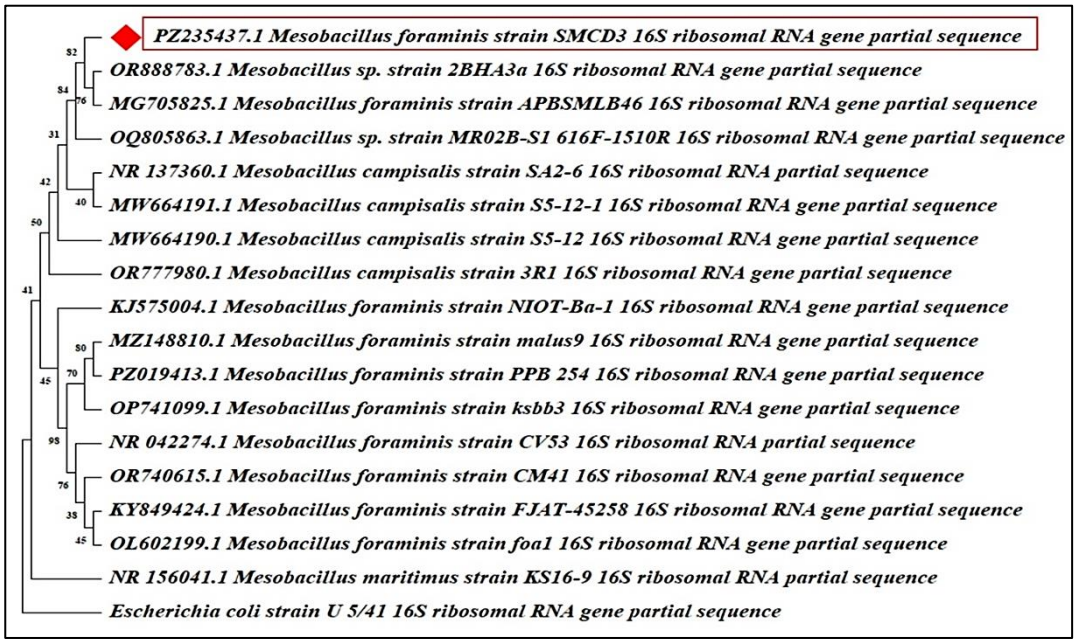

Figure 6. Phylogenetic tree of *MesoBacillus foraminis* strain SMCD3

The growth profile of isolate *MesoBacillus foraminis* strain SMCD3 demonstrated a classical sigmoidal growth pattern under the tested conditions (Figure 7). A distinct lag phase (approximately 0-5 hours) was observed, with negligible OD_{600} variation (0-0.008), indicating physiological adaptation and enzyme synthesis. This was followed by a gradual transition into the exponential phase (approximately 5-8 hours), characterized by a moderate increase in OD_{600} (0.008-0.05). A well-defined exponential phase occurred between approximately 8 and 11 h, with a sharp rise in OD_{600} (0.05-0.114), reflecting rapid cellular proliferation and active metabolism. The culture attained a stationary phase at approximately 24 h, reaching peak biomass ($OD_{600} \approx$ 0.15), likely due to nutrient limitation and accumulation of inhibitory metabolites. Subsequently, a decline phase was observed at 30 h ($OD_{600} \approx 0.12$), indicating reduced cell viability. Overall, optimal growth was achieved at 24 h.

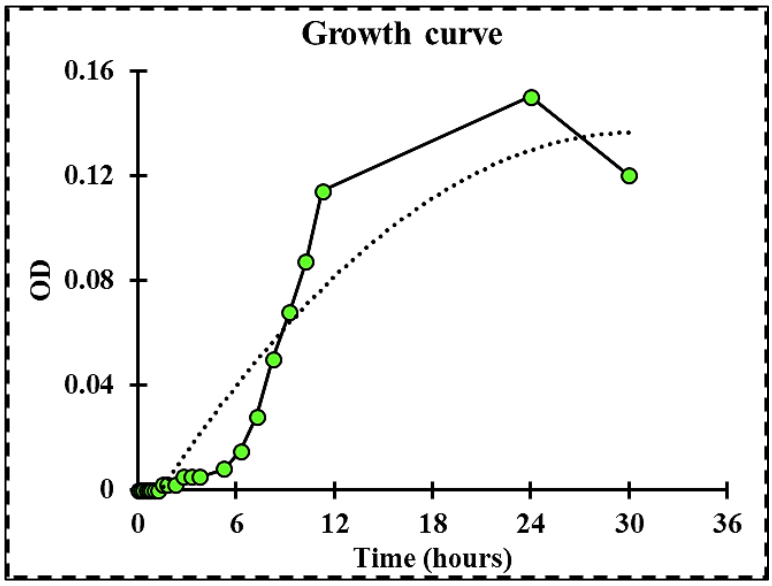

Figure 7. Growth curve of *MesoBacillus foraminis* strain SMCD3

Effect of PS-degrading bacteria on the germination of *Cicer arietinum* exposed to PS-MNPs

PS-MNPs have been increasingly recognized for their adverse effects on terrestrial plants, impacting a wide range of crop species, including onion, carrot, cucumber, mung bean, soybean, rice, and wheat (Kaur et al. 2022; Dong et al. 2021; Huang et al. 2023; Su et al. 2024; Fang et al. 2024). These effects include delayed seed germination, reduced plant growth, impaired photosynthesis, and induction of oxidative stress (Bosker et al. 2019; Zhang et al. 2021; Surgun Acar, 2022). Mechanistically, Li et al. (2020) showed that nanoscale PS particles exhibit enhanced root adsorption, penetration in root tissues, and translocation to aerial parts, leading to accumulation in metabolically active regions and triggering physiological and molecular stress responses.

Similarly, in our study, seedling morphology showed positive effects of *MesoBacillus foraminis* strain SMCD3 in both untreated and PS-MNP-treated seedlings (Figure 8). In this regard, germination parameters such as GP increased by 1.04-fold in the control + SMCD3 treatment compared to the control set, suggesting a mild stimulatory effect of SMCD3 on seed viability under optimal conditions. PS-NP exposure reduced GP to 1.33-fold, indicating substantial inhibition. However, compared to the control group of seedlings, SMCD3 co-application elevated it to 1.037-fold, nearly matching the control. In comparison with the untreated seedlings, PS-MP1 and PS-MP2 treatments showed intermediate reductions of 1.12-fold and 1.22-fold, which improved by 1.037-fold and 1.08-fold, respectively, following SMCD3 inoculation (Figure 9a). Moreover, relative to the corresponding PS-MNPs-treated groups, SMCD3 co-application increased chickpea seed germination by 1.29-, 1.08-, and 1.13-fold under PS-NP, PS-MP1, and PS-MP2 stress conditions, respectively (Figure 9a). These results demonstrate that PS-MNPs adversely affect seed germination, while SMCD3 application substantially alleviates this inhibition, restoring seed viability. SMCD3 consistently improved germination performance across all stress conditions, reaffirming its role as a functional plant growth-promoting bacterium (PGPB) capable of mitigating germination-limiting effects of synthetic pollutants.

Moreover, the control + SMCD3 treatment showed approximately 1.04-fold increase in germination energy over the control, indicating enhanced seed vigour. PS-NP treatment reduced GE to 1.333-fold, while co-treatment with *MesoBacillus foraminis* strain SMCD3 raised it to 1.037-fold compared to the untreated group. Similarly, PS-MP1 and PS-MP2 lowered energy to 1.12-fold and 1.127-fold, which improved with SMCD3 by 1.037-fold and 1.077-fold, respectively, compared to the control set.

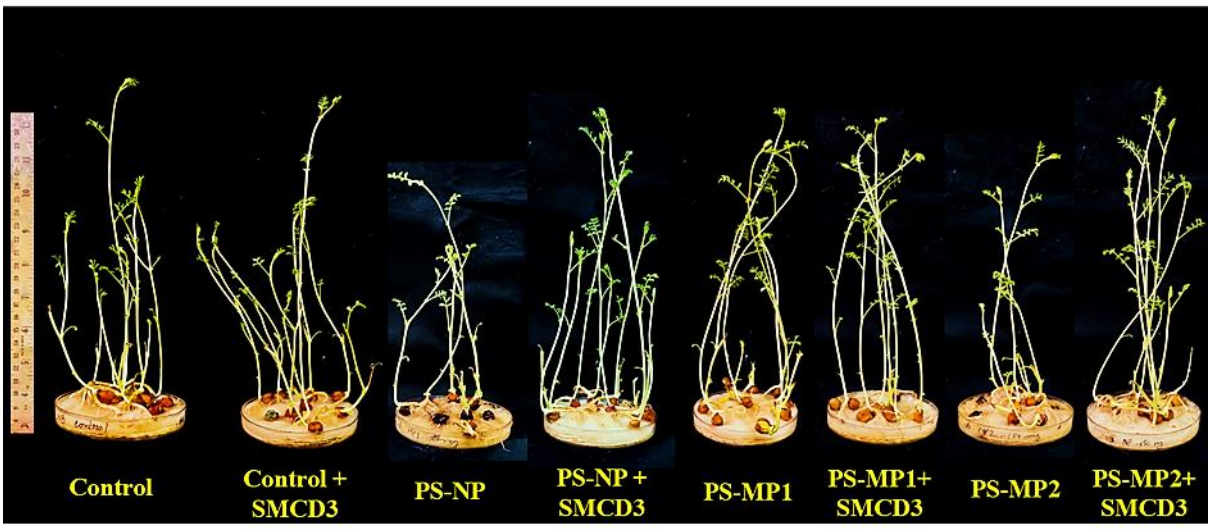

Figure 8. Growth of *Cicer arietinum* under control, control + SMCD3 treatments, PS-MNPs, and PS-MNPs + SMCD3 treatments *MesoBacillus foraminis* strain SMCD3 with the concentration (2.4 mg PS particles/cm2 of Petri dish) of PS-NP – Polystyrene nanoplastic, PS-MP1 – Polystyrene microplastic Type-I, PS-MP2 – Polystyrene microplastic Type-II.

Compared with the corresponding PS-treated groups, SMCD3 co-application enhanced germination energy by 1.29-, 1.08-, and 1.13-fold under PS-NP, PS-MP1, and PS-MP2 stress conditions. These results also show a consistent pattern of reduced vigour due to PS exposure and effective recovery through SMCD3 supplementation. The improvements reflect *M. foraminis* strain SMCD3's ability to restore physiological integrity and uniformity of early seedling growth (Figure 9b). Mean germination time (MGT) was significantly elevated across all PS treatments, indicating delayed germination dynamics under polymer-induced stress. The control + SMCD3 treatment exhibited a moderate increase (1.20-fold) relative to the control, suggesting a slight retardation in germination even under non-stress conditions.

PS-NP exposure resulted in the highest increase in MGT (1.74-fold), reflecting pronounced inhibition of germination rate, which was only marginally alleviated by SMCD3 (1.65-fold). Similarly, PS-MP1 treatment increased MGT (1.55-fold), with no observable mitigation upon *M. foraminis* strain SMCD3 application (Figure 9c). PS-MP2 also induced a substantial delay (1.64-fold), which showed slight improvement in the presence of SMCD3 (1.58-fold). Interestingly, the addition of SMCD3 to PS-stressed seeds resulted in a reduction in MGT under PS-NP and PS-MP2 treatments by 1.06- and 1.04-fold, respectively, relative to the corresponding PS-MNPs treatments alone, whereas MGT remained unchanged under PS-MP1 stress. Collectively, these findings demonstrate that PS particles adversely affect germination kinetics, whereas SMCD3 exhibits limited efficacy in restoring normal germination timing under the tested conditions (Figure 9c). Moreover, the coefficient of velocity of germination (CVG) showed a slight increase (1.06-fold) in the control + SMCD3 treatment compared to the control, indicating a marginal enhancement in germination rate under non-stress conditions. PS-NP exposure caused a substantial decline in CVG (1.87-fold), indicating significant inhibition of germination velocity; however, co-application of SMCD3 effectively restored CVG to near-control levels (1.03-fold) (Figure 9d). PS-MP1 treatment exhibited minimal reduction in CVG (1.08-fold), with negligible improvement following SMCD3 inoculation (1.07-fold). In contrast, PS-MP2 markedly reduced CVG (1.46-fold), which was partially ameliorated by SMCD3 (1.12-fold) (Figure 9d). Moreover, compared with the respective PS-MNPs-stressed treatments, supplementation with *M. foraminis* strain SMCD3 increased the CVG by 1.83-fold under PS-NP stress and 1.30-fold under PS-MP2 stress, while only a marginal induction (1.01-fold) was observed under PS-MP1 stress. Overall, these results indicate that PS-MNPs impair germination kinetics, particularly at the nanoscale, while SMCD3 mitigates these adverse effects by enhancing germination velocity under stress conditions.

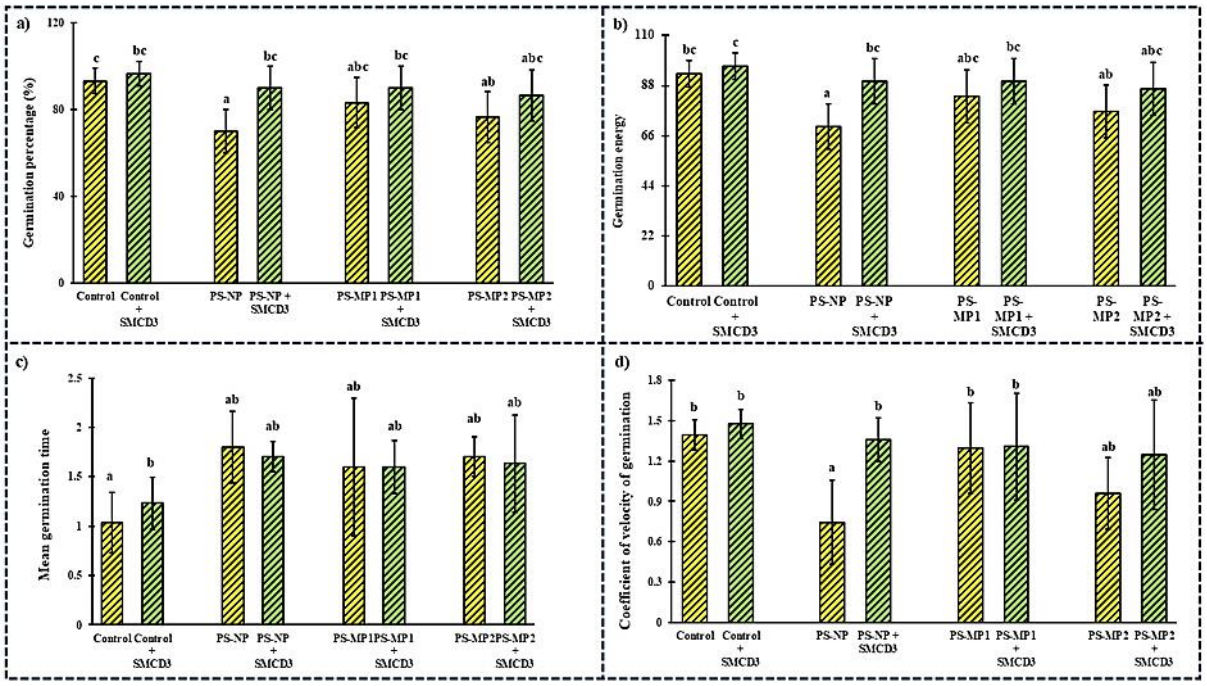

Figure 9. a) Germination percentage, b) Germination energy, c) Mean germination time, and d) Coefficient velocity of germination of *Cicer arietinum* under control, control + SMCD3 treatments, PS-MNPs, and PS-MNPs + SMCD3 treatments *MesoBacillus foraminis* strain SMCD3 with the concentration (2.4 mg PS particles/cm2 of Petri dish) of PS-NP – Polystyrene nanoplastic, PS-MP1 – Polystyrene microplastic Type-I, PS-MP2 – Polystyrene microplastic Type-II. Different letters above the bars indicate statistically significant differences between the mean values (N = 3) of PS-MNPs treatment, as determined by Duncan's test at $p < 0.05$.

Effect of PS-degrading bacteria on the growth parameters of *Cicer arietinum* exposed to PS-MNPs

For growth parameters such as shoot length, the value increased to 1.16-fold in the control + SMCD3 treatment compared to the control, indicating the growth-promoting potential of SMCD3 (Figure 10a). Exposure to PS-NP drastically suppressed shoot length to 2.62-fold, demonstrating severe phytotoxicity. However, co-application with SMCD3 restored shoot length to 1.02-fold, comparable to the control. PS-MP1 and PS-MP2 also negatively affected shoot elongation, reducing it to 1.24-fold and 1.45-fold, respectively. Overall, SMCD3 consistently restored or enhanced shoot elongation across all treatments, with near-complete recovery observed in PS-NP and PS-MP1 co-treated seedlings (Figure 10a). Moreover, the co-application of SMCD3 with PS-MNPs improved shoot elongation compared with the corresponding PS treatments alone. Specifically, shoot length increased by 2.68-, 1.24-, and 1.34-fold under PS-NP, PS-MP1, and PS-MP2 treatments, respectively. Not only that, the root length in the control + SMCD3 group increased slightly to 1.05-fold over the control, confirming that SMCD3 alone supports root development (Figure 10b). PS-NP exposure reduced root length significantly to 2.11-fold, highlighting its inhibitory effect on belowground growth. When SMCD3 was co-applied with PS-NP, root length was restored to 1.00-fold, effectively neutralising the toxic impact. PS-MP1 and PS-MP2 treatments also reduced root length to 1.03-fold and 1.51-fold, respectively. SMCD3 application led to recovery to 1.03-fold (PS-MP1 + SMCD3) and 1.26-fold (PS-MP2 + SMCD3), showing partial remediation. Relative to the respective PS-treated groups, root length was enhanced by 2.12-fold under PS-NP stress and by 1.20-fold under PS-MP2 stress, while root growth remained largely unaffected under PS-MP1 stress. These results demonstrate the ability of *M. foraminis* strain SMCD3 to restore root architecture in *Cicer arietinum* under microplastic stress, reinforcing its utility as a PS-degrading plant growth-promoting bacterium for maintaining root development under plastic-contaminated conditions (Figure 10b).

Leaf surface area increased marginally under control + SMCD3 treatment (1.028-fold) compared to the control. Exposure to PS particles reduced leaf area, with the strongest inhibition observed under PS-NP (2.840-fold), followed by PS-MP2 (1.690-fold) and PS-MP1 (1.203-fold). SMCD3 application effectively alleviated these reductions, restoring leaf area to near-control levels under PS-NP (1.029-fold)

and partially improving it under PS-MP1 (1.183-fold) and PS-MP2 (1.145-fold). Relative to the corresponding PS-treated groups, SMCD3 enhanced leaf surface area by 2.76-, 1.02-, and 1.48-fold under PS-NP, PS-MP1, and PS-MP2 treatments, respectively. Altogether, PS particles negatively impacted leaf expansion, particularly at the nanoscale, while *M. foraminis* strain SMCD3 significantly mitigated these effects, enhancing leaf growth under PS-induced stress conditions (Figure 10c).

Physiological parameters, such as relative water content, increased slightly in the control + SMCD3 treatment (1.038-fold) compared to the control, indicating improved plant water status under non-stress conditions. PS-NP exposure markedly reduced RWC (1.270-fold), whereas SMCD3 restored it to near-control levels (1.010-fold). In contrast, PS-MP1 and PS-MP2 exerted only minor effects on RWC (1.033- and 1.031-fold reductions, respectively), with slight recovery following SMCD3 application (1.024- and 1.023-fold) (Figure 10d). Relative to the corresponding PS-treated groups, SMCD3 increased RWC by 1.26-fold under PS-NP stress, while only marginal improvements (1.01-fold) were observed under PS-MP1 and PS-MP2 treatments. The results of this experiment suggest that PS nanoparticles exerted a greater negative impact on plant water status than microplastics, while *M. foraminis* strain SMCD3 effectively mitigated this stress by maintaining cellular water balance. Moreover, EL, an indicator of membrane damage, increased under PS exposure, reflecting compromised membrane integrity (Figure 10e). SMCD3 treatment alone reduced EL by 1.766-fold relative to the control, indicating enhanced membrane stability under non-stress conditions. PS-NP induced the highest EL (1.716-fold), and SMCD3 exerted only a marginal ameliorative effect (1.676-fold). In contrast, PS-MP1 and PS-MP2 increased EL by 1.480- and 1.612-fold, respectively, whereas SMCD3 markedly reduced leakage to 1.083- and 1.057-fold. Relative to the corresponding PS-treated groups, SMCD3 decreased EL by 2.88-, 1.60-, and 1.70-fold under PS-NP, PS-MP1, and PS-MP2 stress, respectively. These findings demonstrate that while PS induces membrane damage, *M. foraminis* strain SMCD3 more effectively alleviates EL under PS stress.

This study demonstrates the significant phytotoxic effects of PS-MNPs on early seedling development in C. arietinum. PS-NP exposure led to notable alterations in GP, GE, MGT, CVG, shoot and root length, leaf surface area, RWC, and EL. These findings align with established mechanisms by which nanoplastics disrupt plant growth, including physical blockage of water uptake (Figure 8). Such stress responses have been widely reported in contaminated soil systems and are increasingly relevant due to escalating environmental plastic pollution. The bacterial isolate SMCD3 exhibited strong mitigation effects across all parameters, restoring or enhancing seedling performance in both stressed and non-stressed conditions. This bioactivity suggests that SMCD3 possesses multiple plant growth-promoting traits, consistent with those described in plant-beneficial microbes. According to Alves et al. (2022), PGPBs such as *Bacillus*, *Pseudomonas*, *Azospirillum*, and *Rhizobium* contribute to plant stress tolerance by producing phytohormones (e.g., IAA, gibberellins, cytokinins), solubilising nutrients, and modulating ethylene levels through 1-aminocyclopropane-1-carboxylate (ACC) deaminase activity. These mechanisms enable improved germination, root system architecture, biomass allocation, and photosynthetic area under abiotic stress (Alves et al. 2022). The observed recovery in germination metrics (percentage and energy) following SMCD3 inoculation is likely linked to enhanced enzymatic activation and hormonal regulation during early developmental stages. Similarly, improvements in shoot and root length suggest SMCD3-mediated activation of cell division and elongation pathways in the meristematic regions. The enhanced leaf area under plastic stress points to systemic physiological improvements, likely due to increased nutrient uptake via siderophore and organic acid secretion, as described for several PGPB strains in the literature reviewed by Alves et al. (2022). Importantly, SMCD3 also improved growth in control conditions, suggesting a baseline bio-stimulatory capacity. This indicates that beyond bioremediation, SMCD3 could be leveraged as a general biofertilizer. Its dual function-degrading polystyrene and promoting plant growth-makes it a promising tool for integrated strategies addressing both environmental pollution and crop productivity. The enhancement of germination parameters (GP and GE), seedling vigour (shoot and root length), and physiological traits (RWC and reduced EL) in SMCD3-treated plants under PS stress indicates a significant alleviation of PS-induced phytotoxicity. In contrast, PS exposure alone resulted in impaired germination and growth, confirming its inhibitory effects. The improved membrane stability, reflected by decreased electrolyte leakage, suggests mitigation of oxidative damage.

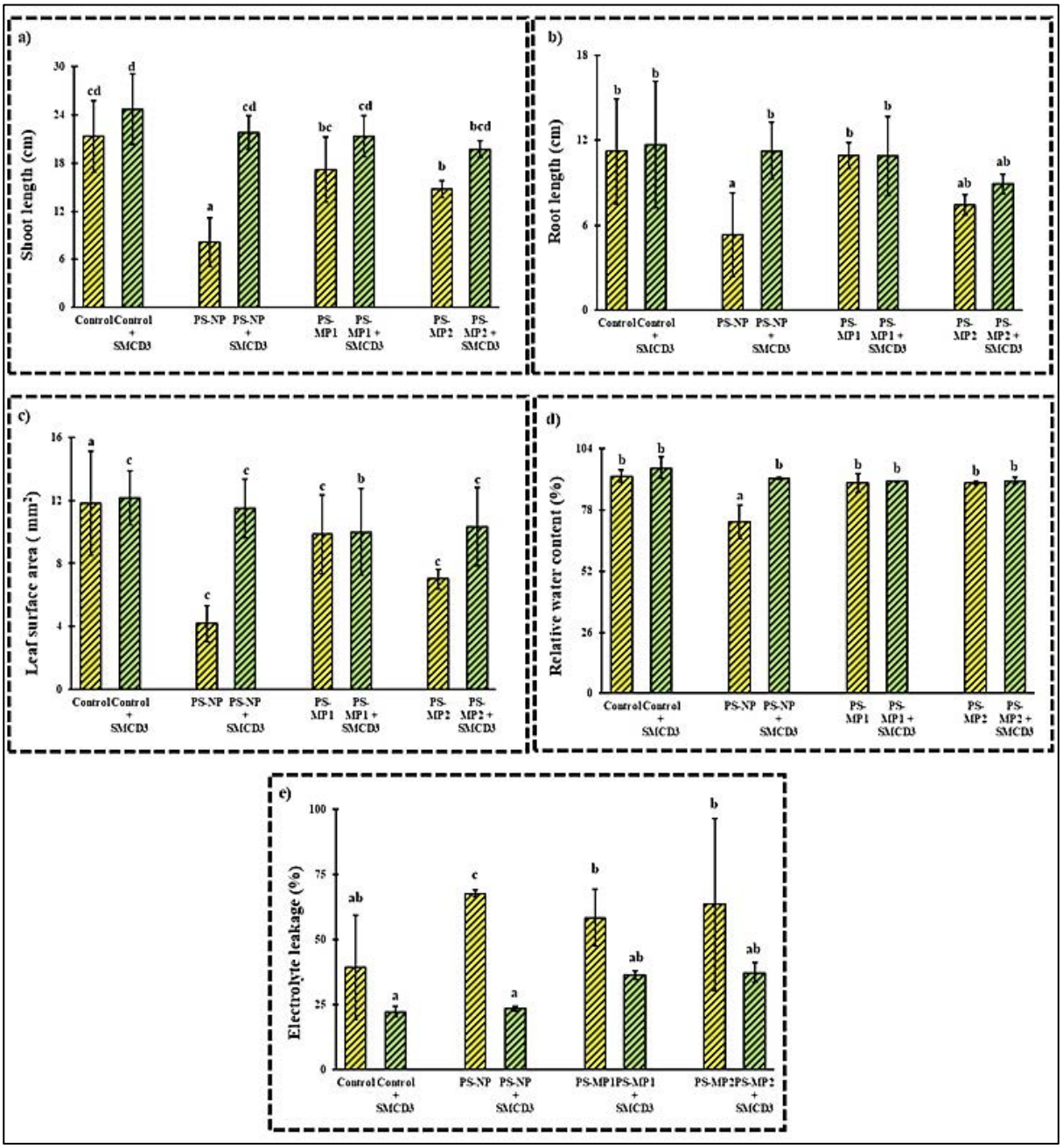

Figure 10. a) Shoot length (cm), b) Root length (cm), c) Leaf surface area (mm2), d) Relative water content, and e) Electrolyte leakage of *Cicer arietinum* under control, control + SMCD3 treatments, PS-MNPs, and PS-MNPs + SMCD3 treatments, *MesoBacillus foraminis* strain SMCD3 with the concentration (2.4 mg PS particles/cm2 of Petri dish) of PS-NP – Polystyrene nanoplastic, PS-MP1 – Polystyrene microplastic Type-I, PS-MP2 – Polystyrene microplastic Type-II. Different letters above the bars indicate statistically significant differences between the mean values (N = 3) of PS-MNPs treatment, as determined by Duncan's test at $p < 0.05$.

These findings are consistent with reported mechanisms where PGPB, such as *Bacillus spizizenii*, enhance plant tolerance to microplastic stress through physiological regulation, improved nutrient acquisition, and stress modulation (Chandel et al. 2025). Thus, SMCD3 demonstrates a dual functional role in promoting plant growth and reducing PS-induced stress.

Conclusion

This study demonstrates that bacterial isolates from municipal dumping ground soil possess significant PS biodegradation potential, with isolate SMCD3 identified as the most efficient strain. Within 6 weeks, SMCD3 exhibited the highest PS weight reduction (14%), coupled with elevated cell density, indicating efficient metabolic assimilation of PS as a sole carbon and energy source under nutrient-limited

conditions. Enzymatic characterization suggests that PS depolymerisation is mediated predominantly through non-classical pathways involving extracellular hydrolases (lipase, esterase) and oxidative enzymes (alkane hydroxylase, alcohol dehydrogenase), rather than laccase- or catechol dioxygenase-dependent aromatic ring cleavage mechanisms. Moreover, SMCD3, more accurately, *MesoBacillus foraminis* strain SMCD3, expressed key plant growth-promoting (PGP) traits, including IAA biosynthesis and utilization, ammonia production, and siderophore secretion, reflecting its potential to enhance rhizospheric nutrient dynamics and phytohormonal regulation. Exposure to PS-MNPs significantly impaired germination kinetics, seedling growth, and physiological integrity of *Cicer arietinum* seedlings. Notably, *M. foraminis* strain SMCD3 inoculation substantially mitigated these phytotoxic effects by restoring germination parameters, improving shoot and root elongation, and enhancing relative water content while reducing membrane damage. Therefore, *M. foraminis* strain SMCD3 represents a metabolically versatile bacterium with dual functional attributes in PS biodegradation and plant growth promotion, underscoring its potential for integrated applications in bioremediation and sustainable agroecosystems under plastic-contaminated conditions.

Acknowledgements

The first author gratefully acknowledges partial financial support from the Swami Vivekananda Merit-cum-Means (SVMCM) Fellowship, Government of West Bengal, India, which facilitated this study. The authors sincerely thank the University of North Bengal for providing essential infrastructure and support for the research. The authors also acknowledge the DST-FIST Facility (Grant No. SR/FST/LS-I/2021/900) and the Department of Botany, University of North Bengal, for granting access to phase-contrast microscopy, which significantly contributed to the completion of this work.

Funding

The first author acknowledges partial financial support from the SVMCM Fellowship, Government of West Bengal, India, which contributed to the execution of this study.

Competing interests

The authors declare the absence of any known competing financial interests or personal relationships that could have influenced the conception, methodology, analysis, or interpretation of the reported findings.

References

Abbas-Abadi, M.S., 2021. The effect of process and structural parameters on the stability, thermo-mechanical and thermal degradation of polymers with hydrocarbon skeleton containing PE, PP, PS, PVC, NR, PBR and SBR. Journal of Thermal Analysis and Calorimetry, 143(4), pp.2867-2882. DOI: https://doi.org/10.1007/s10973-020-09344-0.

Abdelmoteleb, A., Troncoso-Rojas, R., Gonzalez-Soto, T. and González-Mendoza, D., 2017. Antifungical activity of autochthonous *Bacillus subtilis* isolated from Prosopis juliflora against phytopathogenic fungi. Mycobiology, 45(4), pp.385-391. DOI: https://doi.org/10.5941/MYCO.2017.45.4.385.

Abirami, G., Srimathi, M., Suganthi, M., Ramprasath, C. and Manjunathan, J., 2021. Plastic Degrading Ability of Laccase Enzyme Isolated From Garbage Dumping Sites of Chennai. Poll Res, 40(1), pp.199-202. DOI: https://doi.org/10.1098/RSTB.2009.0053.

Aboryia, M., AL-Saoud, A.M.A., El-Boraie, E.S.A., Abd El-Gawad, H.G., Ismail, S., Alkafafy, M., Aljuaid, B.S. and Abu-Ziada, L.M., 2024. Seed germination, seedling growth performance, genetic stability and biochemical responses of papaya (Carica papaya L.) upon pre-sowing seed treatments. Folia Hort, 36(4), pp.533-558. DOI: 10.2478/fhort-2024-0036.

Afrin, S., Tamanna, T., Shahajadi, U.F., Bhowmik, B., Jui, A.H., Miah, M.A.S. and Bhuiyan, M.N.I., 2024. Characterization of protease-producing bacteria from garden soil and antagonistic activity against pathogenic bacteria. The Microbe, 4, p.100123. DOI: https://doi.org/10.1016/j.microb.2024.100123.

Aktas, E., Yigit, N. and Ayyildiz, A., 2002. Esterase activity in various Candida species. Journal of international medical research, 30(3), pp.322-324. DOI: https://doi.org/10.1177/14732300020300031

Alström, S. and Burns, R.G., 1989. Cyanide production by rhizobacteria as a possible mechanism of plant growth inhibition. Biology and Fertility of Soils, 7(3), pp.232-238. DOI: https://doi.org/10.1007/BF00709654.

Alves, A.R., Yin, Q., Oliveira, R.S., Silva, E.F. and Novo, L.A., 2022. Plant growth-promoting bacteria in phytoremediation of metal-polluted soils: Current knowledge and future directions.

Science of the Total Environment, 838, p.156435. DOI: https://doi.org/10.1016/j.scitotenv.2022.156435.

Asmita, K., Shubhamsingh, T. and Tejashree, S., 2015. Isolation of plastic degrading micro-organisms from soil samples collected at various locations in Mumbai, India. International Research Journal of Environment Sciences, 4(3), pp.77-85.

Barr, H.D. and Weatherley, P.E., 1962. A re-examination of the relative turgidity technique for estimating water deficit in leaves. Aust. J. Biol. Sci, 15(3), pp.413-428. DOI: https://doi.org/ 10.1071/BI9620413.

Bhatt, S., Dholakia, P.R., Sorathia, D.K., Solanki, K.J., Dabhi, N.K. and Dedakiya, S.K., 2015. Isolation & biochemical characterization of halotolerant plant growth promoting rhizobacteria. DOI: http://10.9.150.37:8080/dspace//handle/atmiyauni/911.

Bhattacharyya, P.N. and Jha, D.K., 2012. Plant growth-promoting rhizobacteria (PGPR): emergence in agriculture. World Journal of Microbiology and Biotechnology, 28, pp.1327-1350. DOI: https://doi.org/10.1007/s11274-011-0979-9.

Bidashimwa, D., Hoke, T., Huynh, T.B., Narkpitaks, N., Priyonugroho, K., Ha, T.T., Burns, A. and Weissman, A., 2023. Plastic pollution: how can the global health community fight the growing problem?. BMJ Global Health, 8(Suppl 3), p.e012140. DOI: 10.1136/bmjgh-2023-012140.

Bochner, B.R. and Savageau, M.A., 1977. Generalized indicator plate for genetic, metabolic, and taxonomic studies with microorganisms. Applied and Environmental Microbiology, 33(2), pp.434-444. DOI: https://doi.org/10.1128/aem.33.2.434-444.1977.

Bosker, T., Bouwman, L.J., Brun, N.R., Behrens, P. and Vijver, M.G., 2019. Microplastics accumulate on pores in seed capsule and delay germination and root growth of the terrestrial vascular plant Lepidium sativum. Chemosphere, 226, pp.774-781. DOI: https://doi.org/10.1016/j.chemosphere.2019.03.163.

Bric, J.M., Bostock, R.M. and Silverstone, S.E., 1991. Rapid in situ assay for indoleacetic acid production by bacteria immobilized on a nitrocellulose membrane. Applied and environmental Microbiology, 57(2), pp.535-538. https://doi.org/10.1128/aem.57.2.535-538.1991.

Chandel, R., Chauhan, S., Devi, S. and Thakur, S., 2025. Polystyrene microplastic degradation by a novel PGPR *Bacillus* spizizenii. Journal of Hazardous Materials, 491, p.137892. DOI: https://doi.org/10.1016/j.jhazmat.2025.137892

Chaudhary, A.K., Chaitanya, K. and Vijayakumar, R.P., 2021. Synergistic effect of UV and chemical treatment on biological degradation of Polystyrene by Cephalosporium strain NCIM 1251. Archives of Microbiology, 203(5), pp.2183-2191. DOI: https://doi.org/10.1007/s00203-021-02228-3.

Christensen, W.B., 1946. Urea decomposition as a means of differentiating Proteus and paracolon cultures from each other and from Salmonella and Shigella types. Journal of bacteriology, 52(4), pp.461-466. DOI: 10.1128/jb.52.4.461-466.1946.

de la Cruz, T.E.E. and Torres, J.M.O., Gelatin hydrolysis test protocol. American Society for Microbiology; 2012.

Dey, S., Guha, T., Barman, F., Natarajan, L., Kundu, R., Mukherjee, A. and Paul, S., 2023. Surface functionalization and size of polystyrene microplastics concomitantly regulate growth, photosynthesis and anti-oxidant status of *Cicer arietinum* L. Plant Physiology and Biochemistry, 194, pp.41-51. DOI: https://doi.org/10.1016/j.plaphy.2022.11.004.

Dong, Y., Gao, M., Qiu, W. and Song, Z., 2021. Uptake of microplastics by carrots in presence of As (III): Combined toxic effects. Journal of Hazardous Materials, 411, p.125055. DOI: https://doi.org/10.1016/j.jhazmat.2021.125055

Duan, J., Bolan, N., Li, Y., Ding, S., Atugoda, T., Vithanage, M., Sarkar, B., Tsang, D.C. and Kirkham, M.B., 2021. Weathering of microplastics and interaction with other coexisting constituents in terrestrial and aquatic environments. Water Research, 196, p.117011. DOI: https://doi.org/10.1016/j.watres.2021.117011.

Etesami, H. and Glick, B.R., 2024. Bacterial indole-3-acetic acid: A key regulator for plant growth, plant-microbe interactions, and agricultural adaptive resilience. Microbiological Research, 281, p.127602. DOI: https://doi.org/10.1016/j.micres.2024.127602.

Fang, X.Z., Fang, S.Q., Ding, Y., Ma, J.W., Ye, Z.Q., Liu, D. and Zhao, K.L., 2024. Microplastic exposure inhibits nitrate uptake and assimilation in wheat plants.

Environmental Pollution, 360, p.124626. DOI: https://doi.org/10.1016/j.envpol.2024.124626.

Feng, Y., Tian, B., Xiong, J., Lin, G., Cheng, L., Zhang, T., Lin, B., Ke, Z. and Li, X., 2024. Exploring IAA biosynthesis and plant growth promotion mechanism for tomato root endophytes with incomplete IAA synthesis pathways. Chemical and Biological Technologies in Agriculture, 11(1), p.187. DOI: https://doi.org/10.1186/s40538-024-00712-8.

Fuchs, G., Boll, M. and Heider, J., 2011. Microbial degradation of aromatic compounds-from one strategy to four. Nature Reviews Microbiology, 9(11), pp.803-816. DOI: https://doi.org/10.1038/nrmicro2652.

Geyer, R., Jambeck, J.R. and Law, K.L., 2017. Production, use, and fate of all plastics ever made. Science advances, 3(7), p.e1700782. DOI: 10.1126/sciadv.1700782.

Gutberlet, J., 2023. Global plastic pollution and informal waste pickers. Cambridge Prisms: Plastics, 1, p.e9. DOI: https://doi.org/10.1017/plc.2023.10.

Hou, L. and Majumder, E.L.W., 2021. Potential for and distribution of enzymatic biodegradation of polystyrene by environmental microorganisms. Materials, 14(3), p.503. DOI: https://doi.org/10.3390/ma14030503.

Huang, D., Shi, Z., Shan, X., Yang, S., Zhang, Y. and Guo, X., 2023. Insights into growth-affecting effect of nanomaterials: Using metabolomics and transcriptomics to reveal the molecular mechanisms of cucumber leaves upon exposure to polystyrene nanoplastics (PSNPs). Science of The Total Environment, 866, p.161247. DOI: https://doi.org/10.1016/j.scitotenv.2022.161247.

Karkanorachaki, K., Tsiota, P., Dasenakis, G., Syranidou, E. and Kalogerakis, N., 2022. Nanoplastic generation from secondary PE microplastics: microorganism-induced fragmentation. Microplastics, 1(1), pp.85-101. DOI: https://doi.org/10.3390/microplastics1010006.

Kaur, M., Xu, M. and Wang, L., 2022. Cyto–genotoxic effect causing potential of polystyrene micro-plastics in terrestrial plants. Nanomaterials, 12(12), p.2024.

DOI: https://doi.org/10.3390/nano12122024.

Khatoon, H., Anokhe, A. and Kalia, V., 2022. Catalase test: A biochemical protocol for bacterial identification. AgriCos e-Newsletter, 3(1), pp.53-55.

Khodadadi, H., Eghtedarnejad, E., Ahmadi, A., Khodadadi, A. and Shamsdin, N., 2025. Evaluation of usage of readily accessible Enterobacteriaceae differential and selective media for identifying Candida auris. Diagnostic Microbiology and Infectious Disease, 111(1), p.116589. DOI: https://doi.org/10.1016/j.diagmicrobio.2024.116589.

Kim, H.W., Jo, J.H., Kim, Y.B., Le, T.K., Cho, C.W., Yun, C.H., Chi, W.S. and Yeom, S.J., 2021. Biodegradation of polystyrene by bacteria from the soil in common environments. Journal of Hazardous Materials, 416, p.126239. DOI: https://doi.org/10.1016/j.jhazmat.2021.126239

Kloos, K., Munch, J.C. and Schloter, M., 2006. A new method for the detection of alkane-monooxygenase homologous genes (alkB) in soils based on PCR-hybridization. Journal of Microbiological Methods, 66(3), pp.486-496. https://doi.org/10.1016/j.mimet.2006.01.014.

Kukharchyk, T.I. and Chernyk, V.D., 2022. Soil pollution with microplastic in the impact area of a plant producing expanded polystyrene. Eurasian Soil Science, 55(3), pp.377-386. DOI: https://doi.org/10.1134/S1064229322030085.

Kulkarni, M.G., Street, R.A. and Van Staden, J., 2007. Germination and seedling growth requirements for propagation of Dioscorea dregeana (Kunth) Dur. and Schinz—A tuberous medicinal plant. South African Journal of Botany, 73(1), pp.131-137. DOI: https://doi.org/10.1016/j.sajb.2006.09.002.

Lal, A. and Cheeptham, N., 2012. Starch agar protocol. American Society for Microbiology, 1, pp.1-9.

Leveau, J.H. and Lindow, S.E., 2005. Utilization of the plant hormone indole-3-acetic acid for growth by Pseudomonas putida strain 1290. Applied and environmental microbiology, 71(5), pp.2365-2371. DOI: https://doi.org/10.1128/AEM.71.5.2365-2371.2005

Li, L., Luo, Y., Li, R., Zhou, Q., Peijnenburg, W.J., Yin, N., Yang, J., Tu, C. and Zhang, Y., 2020. Effective uptake of submicrometre plastics by crop plants via a crack-entry mode. Nature sustainability, 3(11), pp.929-937. DOI: https://doi.org/10.1038/s41893-020-0567-9

Li, Z., Li, R., Li, Q., Zhou, J. and Wang, G., 2020. Physiological response of cucumber (Cucumis sativus L.) leaves to polystyrene nanoplastics pollution. Chemosphere, 255, p.127041. DOI:

https://doi.org/10.1016/j.chemosphere.2020.127041.

Liu, Y.Q., Chen, Y., Ren, X.M., Li, Y.Y., Zhang, Y.J., Zhang, H., Han, H. and Chen, Z.J., 2023. Plant growth-promoting bacteria modulate gene expression and induce antioxidant tolerance to alleviate synergistic toxicity from combined microplastic and Cd pollution in sorghum. Ecotoxicology and Environmental Safety, 264, p.115439. DOI: https://doi.org/10.1016/j.ecoenv.2023.115439.

Lutts, S., Kinet, J.M. and Bouharmont, J., 1996. NaCl-induced senescence in leaves of rice (Oryza sativa L.) cultivars differing in salinity resistance. Annals of botany, 78(3), pp.389-398. DOI: https://doi.org/10.1006/anbo.1996.0134.

Maneesha, M. and Subathra Devi, C., 2026. Statistical optimization of fermentation conditions for enhanced production of Nattokinase from *Bacillus subtilis* MM26. BMC biotechnology. DOI: https://doi.org/10.1186/s12896-025-01093-y.

Marquez, C., Martin, C., Linares, N. and De Vos, D., 2023. Catalytic routes towards polystyrene recycling. Materials horizons, 10(5), pp.1625-1640. DOI: 10.1039/D2MH01215D.

Minhas, W.R., Bashir, S., Zhang, C. and Raza, A., 2025. Optimized production of laccase from Pseudomonas stutzeri and its biodegradation of lignin in biomass. Folia Microbiologica, 70(5), pp.1043-1050. DOI: https://doi.org/10.1007/s12223-024-01232-6.

Mohan, A.J., Sekhar, V.C., Bhaskar, T. and Nampoothiri, K.M., 2016. Microbial assisted high impact polystyrene (HIPS) degradation. Bioresource technology, 213, pp.204-207. https://doi.org/10.1016/j.biortech.2016.03.021

Mohanan, N., Montazer, Z., Sharma, P.K. and Levin, D.B., 2020. Microbial and enzymatic degradation of synthetic plastics. Frontiers in Microbiology, 11, p.580709. DOI: https://doi.org/10.3389/fmicb.2020.580709.

Muthukumar, J., Kandukuri, V.A. and Chidambaram, R., 2024. A critical review on various treatment, conversion, and disposal approaches of commonly used polystyrene. Polymer Bulletin, 81(4), pp.2819-2845. DOI: https://doi.org/10.1007/s00289-023-04851-0.

Mzibra, A., Aasfar, A., Benhima, R., Khouloud, M., Boulif, R., Douira, A., Bamouh, A. and Meftah Kadmiri, I., 2021. Biostimulants derived from Moroccan seaweeds: seed germination metabolomics and growth promotion of tomato plant. Journal of Plant Growth Regulation, 40(1), pp.353-370. DOI: https://doi.org/10.1007/s00344-020-10104-5.

Nahar, N., 1994. Characterization of activated sludge bacteria capable of growth on toluene and other aromatic compounds (Doctoral dissertation, Dublin City University).

Olagunju, O.O., Ogunnusi, T.A. and Akpor, O.B., 2025. Evaluation of Indole acetic acid and hydrogen cyanide production by plant growth promoting rhizobacteria. Vegetos, pp.1-8. DOI: https://doi.org/10.1007/s42535-025-01347-2.

Oyewusi, H.A., Wahab, R.A., Kaya, Y., Edbeib, M.F. and Huyop, F., 2020. Alternative bioremediation agents against haloacids, haloacetates and chlorpyrifos using novel halogen-degrading bacterial isolates from the hypersaline lake Tuz. Catalysts, 10(6), p.651.DOI: https://doi.org/10.3390/catal10060651.

Özdemir, S., Akarsu, C., Acer, Ö., Fouillaud, M., Dufossé, L. and Dizge, N., 2022. Isolation of thermophilic bacteria and investigation of their microplastic degradation ability using polyethylene polymers. Microorganisms, 10(12), p.2441. DOI: https://doi.org/10.3390/microorganisms10122441.

Parthasarathy, A., Miranda, R.R., Eddingsaas, N.C., Chu, J., Freezman, I.M., Tyler, A.C. and Hudson, A.O., 2022. Polystyrene degradation by Exiguobacterium sp. RIT 594: preliminary evidence for a pathway containing an atypical oxygenase. Microorganisms, 10(8), p.1619. https://doi.org/10.3390/microorganisms10081619.

Pikovskaya, R.I. 1948. Mobilization of phosphorus in soil in connection with the vital activity of some microbial species. Mikrobiologiya 17: 362-370.

Rao, M.B., Tanksale, A.M., Ghatge, M.S. and Deshpande, V.V., 1998. Molecular and biotechnological aspects of microbial proteases. Microbiology and molecular biology reviews, 62(3), pp.597-635. DOI: https://doi.org/10.1128/mmbr.62.3.597-635.1998.

Reiner, K., 2012. Carbohydrate fermentation protocol. energy, 11, p.12.

Restrepo-Flórez, J.M., Bassi, A. and Thompson, M.R., 2014. Microbial degradation and deterioration of polyethylene–A review. International Biodeterioration & Biodegradation, 88, pp.83-90. DOI: https://doi.org/10.1016/j.ibiod.2013.12.014.

Salihu, A., Alam, Z., AbdulKarim, M.I. and Salleh, H.M., 2011. Suitability of using palm oil mill effluent as a medium for lipase production. African Journal of Biotechnology, 10(11), pp.2044-2052.

Šaraba, V., Milovanovic, J., Nikodinovic-Runic, J., Budin, C., de Boer, T. and Ciric, M., 2023. Brackish groundwaters contain plastic-and cellulose-degrading bacteria. Microbial Ecology, 86(4), pp.2747-2755. DOI: https://doi.org/10.1007/s00248-023-02278-8.

Scott, S.J., Jones, R.A. and Williams, W., 1984. Review of data analysis methods for seed germination 1. Crop science, 24(6), pp.1192-1199. DOI: https://doi.org/10.2135/cropsci1984.0011183X002400060043x.

Sharma, A.K., Gupta, J.S. and Dixit, R.B., 1986. Incidence of pathogenic conidia on leaf surface of yellow sarson and taramira.

Srinivasan, D., Girish, V., Kumbipalya Narayan, V.S., Patel, I.D., Thimmappa, V., Sarvepalli, K., Madhavan, J.K. and Ravi, L., 2025. Microbacterium thalassium VALIDK02: an indole-3-acetic-acid producing endophyte of Capsicum frutescens as a promising biofertilizer for agricultural applications. Discover Plants, 2(1), p.259. DOI: https://doi.org/10.1007/s44372-025-00344-8.

Su, D., Li, W., Zhang, Z., Cai, H., Zhang, L., Sun, Y., Liu, X. and Tian, Z., 2024. Discrepancy of Growth Toxicity of Polystyrene Nanoplastics on Soybean (Glycine max) and Mung Bean (Vigna radiata). Toxics, 12(2), p.155.

DOI: https://doi.org/10.3390/toxics12020155.

Surgun-Acar, Y., 2022. Response of soybean (Glycine max L.) seedlings to polystyrene nanoplastics: Physiological, biochemical, and molecular perspectives. Environmental Pollution, 314, p.120262. DOI: https://doi.org/10.1016/j.envpol.2022.120262.

Tan, K.M., Fauzi, N.A.M., Kassim, A.S.M. and Rehan, A.M., 2022. Enhancing SDS-PAGE detection of dilute extracellular polystyrene degrading enzymes expressed by *Bacillus* megaterium strain via centrifugal freeze concentration method. Trends in Sciences, 19(15), pp.5613-5613. DOI: https://doi.org/10.48048/tis.2022.5613.

Taylor, S.E., Pearce, C.I., Sanguinet, K.A., Hu, D., Chrisler, W.B., Kim, Y.M., Wang, Z. and Flury, M., 2020. Polystyrene nano-and microplastic accumulation at Arabidopsis and wheat root cap cells, but no evidence for uptake into roots. Environmental Science: Nano, 7(7), pp.1942-1953. DOI: https://doi.org/10.1039/d0en00309c.

Tesso, T.A. and Liu, G., 2019. Indole degradation in a model system and in poultry manure by Acinetobacter spp. Applied Sciences, 9(8), p.1622. https://doi.org/10.3390/app9081622.

Timofeeva, A.M., Galyamova, M.R. and Sedykh, S.E., 2023. Plant growth-promoting soil bacteria: nitrogen fixation, phosphate solubilization, siderophore production, and other biological activities. Plants, 12(24), p.4074.https://doi.org/10.3390/plants12244074.

Toghueo, R.M., Zabalgogeazcoa, I., de Aldana, B.V. and Boyom, F.F., 2017. Enzymatic activity of endophytic fungi from the medicinal plants Terminalia catappa, Terminalia mantaly and Cananga odorata. South African Journal of Botany, 109, pp.146-153. DOI: https://doi.org/10.1016/j.sajb.2016.12.021.

Ugueri, U., Atuanya, E.I. and Zainab, U., 2022. Biodegradability of polystyrene plastics by bacterial isolates from plastic composted waste soil and molecular characterization of plastic degrading bacterial isolates. African Journal of Microbiology Research, 16(6), pp.247-257. https://doi.org/10.5897/AJMR2020.9341.

Ullah, A., Sadaf, S., Ullah, S., Alshaya, H., Okla, M.K., Alwasel, Y.A. and Tariq, A., 2022. Using halothermal time model to describe barley (Hordeumvulgare L.) seed germination response to water potential and temperature. Life, 12(2), p.209. DOI: https://doi.org/10.3390/life12020209.

Urbanek, A.K., Rymowicz, W. and Mirończuk, A.M., 2018. Degradation of plastics and plastic-degrading bacteria in cold marine habitats. Applied microbiology and biotechnology, 102, pp.7669-7678. DOI: https://doi.org/10.1007/s00253-018-9195-y.

Wang, L., Liu, Y., Kaur, M., Yao, Z., Chen, T. and Xu, M., 2021. Phytotoxic effects of polyethylene microplastics on the growth of food crops soybean (Glycine max) and mung bean (Vigna radiata). International journal of environmental research and public health, 18(20), p.10629.https://doi.org/10.3390/ijerph182010629.

Wilkes, R.A. and Aristilde, L., 2017. Degradation and metabolism of synthetic plastics and associated products by Pseudomonas sp.: capabilities and challenges. Journal of applied microbiology, 123(3), pp.582-593. DOI: https://doi.org/10.1111/jam.13472.

Xiang, P., Zhang, Y., Zhang, T., Wu, Q., Zhao, C. and Li, Q., 2023. A novel bacterial combination for efficient degradation of polystyrene microplastics. Journal of Hazardous Materials, 458, p.131856. DOI: https://doi.org/10.1016/j.jhazmat.2023.131856

Xiao, Y., Tian, Y., Xu, W. and Zhu, J., 2024. Photodegradation of microplastics through nanomaterials: Insights into photocatalysts modification and detailed mechanisms. Materials, 17(11), p.2755. DOI: https://doi.org/10.3390/ma17112755.

Xu, Y., Ou, Q., van der Hoek, J.P., Liu, G. and Lompe, K.M., 2024. Photo-oxidation of micro- and nanoplastics: physical, chemical, and biological effects in environments. Environmental science & technology, 58(2), pp.991-1009. DOI: https://doi.org/10.1021/acs.est.3c07035.

Yan, H., Cordier, M. and Uehara, T., 2024. Future projections of global plastic pollution: Scenario analyses and policy implications. Sustainability, 16(2), p.643. DOI: https://doi.org/10.3390/su16020643.

Yoon, M.G., Jeon, H.J. and Kim, M.N., 2012. Biodegradation of polyethylene by a soil bacterium and AlkB cloned recombinant cell. J Bioremed Biodegrad, 3(4), pp.1-8. DOI: 10.4172/2155-6199.1000145.

Yousif, E. and Haddad, R., 2013. Photodegradation and photostabilization of polymers, especially polystyrene. SpringerPlus, 2(1), p.398. DOI: https://doi.org/10.1186/2193-1801-2-398.

Zhang, Q., Zhao, M., Meng, F., Xiao, Y., Dai, W. and Luan, Y., 2021. Effect of polystyrene microplastics on rice seed germination and antioxidant enzyme activity. Toxics, 9(8), p.179. DOI: https://doi.org/10.3390/toxics9080179.

Zhang, S., Deng, Z., Borham, A., Ma, Y., Wang, Y., Hu, J., Wang, J. and Bohu, T., 2023. Significance of soil siderophore-producing bacteria in evaluation and elevation of crop yield. Horticulturae, 9(3), p.370. DOI: https://doi.org/10.3390/horticulturae9030370.

Zimmermann, J., Kruppa, D., Fischlschweiger, M., Beuermann, S. and Enders, S., 2021. Ultrasonic degradation of polystyrene for tailoring molecular weight and polydispersity of polystyrene fragments. Chemie Ingenieur Technik, 93(1-2), pp.289-296. DOI: https://doi.org/10.1002/cite.202000119.